American Mineralogist, Volume 95, pages 1478–1492, 2010

Primary Nb-Ta minerals in the Szklary pegmatite, Poland: New insights into controls of crystal chemistry and crystallization sequences

ADAM PIECZKA*

Department of Mineralogy, Petrography and Geochemistry, AGH, University of Science and Technology, Mickiewicza 30, 30-059 Kraków, Poland

ABSTRACT

An assemblage of primary, extremely As- and Sb-rich, Nb-Ta minerals from the Szklary pegmatite includes columbite-(Fe), columbite-(Mn), tantalite-(Mn), stibiocolumbite, stibiotantalite, an as yet unnamed (As,Sb,U)-rich (Ta,Ti)-oxide, $Mn_3UAs_2Sb_2Ta_2Ti_2O_{20}$, and holtite. Anomalous trends of Mn-Fe and Ta-Nb fractionation in the columbite group and crystallization sequences in the primary assemblage can be explained by the contamination of the pegmatite-forming melt by ultramafic and mafic wall-rocks, the competition among these minerals for Ta and Sb and with biotite and tourmaline for Mg, Fe, and Ti, and local variations in melt composition. A hot magmatic fluid, exsolved from the parental melt, reacted with the primary Nb-Ta oxides, inducing two different patterns of alteration. The columbite-group minerals were altered to fersmite, pyrochlore, and bismutopyrochlore locally grading to plumbopyrochlore, whereas stibiocolumbite, stibiotantalite, and the (As,Sb,U)-rich (Ta,Ti)-oxide altered to stibiomicrolite, uranmicrolite grading to betafite, and then to bismutomicrolite or Bi-dominant betafite. In all of the secondary pyrochlore-group minerals, Ta-Nb fractionation is comparable to, or only slightly greater, than that in the primary Nb-Ta oxides, indicating a modest differentiation of the residual melt coexisting with the fluid.

Keywords: Columbite-(Fe), columbite-(Mn), tantalite-(Mn), stibiocolumbite, stibiotantalite, holtite, fersmite, pyrochlore-group minerals, fractionation trends, Szklary pegmatite, Lower Silesia, Poland

INTRODUCTION

A pegmatite dike hosted by serpentinite in the Szklary massif is exposed over a small area (about 4 × 1 m), but can be recognized as a unique mineral locality worldwide due to the presence of several previously unidentified phases and an assemblage of extremely As-, Sb-, and Bi-rich Nb-Ta minerals. The dike hosts such rare minerals as holtite, stibiocolumbite, stibiotantalite, paradocrasite, stibarsen, Mn-rich beusite, Mn-rich fluorapatite, hydroxylapatite, and chlorapatite, as well as previously unknown phases such as $Mn_3Ca_2(PO_4)_3Cl$ (Pieczka 2007a), and Ba- and Pb-dominant analogues of dickinsonite (arrojadite group), $MnAs_2O_4$, $Al_4As_2O_9$, and $Mn_3UAs_2Sb_2Ta_2Ti_2O_{20}$. In addition to the Nb-Ta minerals, various members of the columbite group, fersmite and the pyrochlore-, microlite-, and betafite-subgroups of the pyrochlore group have been recognized. Very few of these minerals have been adequately characterized to date; there are only brief descriptions of columbite-(Mn) and stibiocolumbite (Pieczka et al. 1997), holtite (Pieczka and Marszałek 1996), and pyrochlore (Pieczka and Gołębiowska 2001).

The aim of the current study is to provide a complete description of the primary Nb-Ta minerals present in the pegmatite with emphasis on the chemical conditions of their crystallization and their temporal and paragenetic relationships. The results presented here are the first comprehensive summary of the parameters that control crystallization of the Nb-Ta oxides and holtite in the Szklary pegmatite.

GEOLOGICAL SETTING

The Szklary massif is situated about 60 km south of Wrocław and 6 km north of Ząbkowice Śląskie in the southern part of the Mississippian Niemcza shear zone (Fig. 1). The zone extends along the eastern edge of the Góry Sowie block in the northeastern part of the Bohemian Massif (the Central Sudetes and the Fore-Sudetic block, southwestern Poland). The massif is one of several small bodies of serpentinized ultramafic and mafic rocks that rim the Góry Sowie gneissic complex and are considered to be parts of a tectonically fragmented Sudetic ophiolite suite (Majerowicz and Pin 1986) about 420 Ma old (Oliver et al. 1993). According to Żelaźniewicz (1990), the Góry Sowie complex and the Sudetic ophiolite were already in contact in the Late Devonian. The massif is composed of weakly serpentinized harzburgites, lherzolites, and pyroxenites containing enclaves of amphibolites and rodingites. The serpentinites are crosscut by numerous aplite, and less commonly, lamprophyre veins in the northern and central parts of the massif. The Szklary pegmatite dike, is the only known dike from the northern part of the massif, where it is exposed in one of the open pits in an abandoned silicate nickel mine. The pegmatite dike represents the rare earth element (REE) subclass of the muscovite-rare earth element (MSREL) pegmatite class in the classification of Černý and Ercit (2005).

* E-mail: pieczka@agh.edu.pl

0003-004X/10/0010–1478$05.00/DOI: 10.2138/am.2010.3321

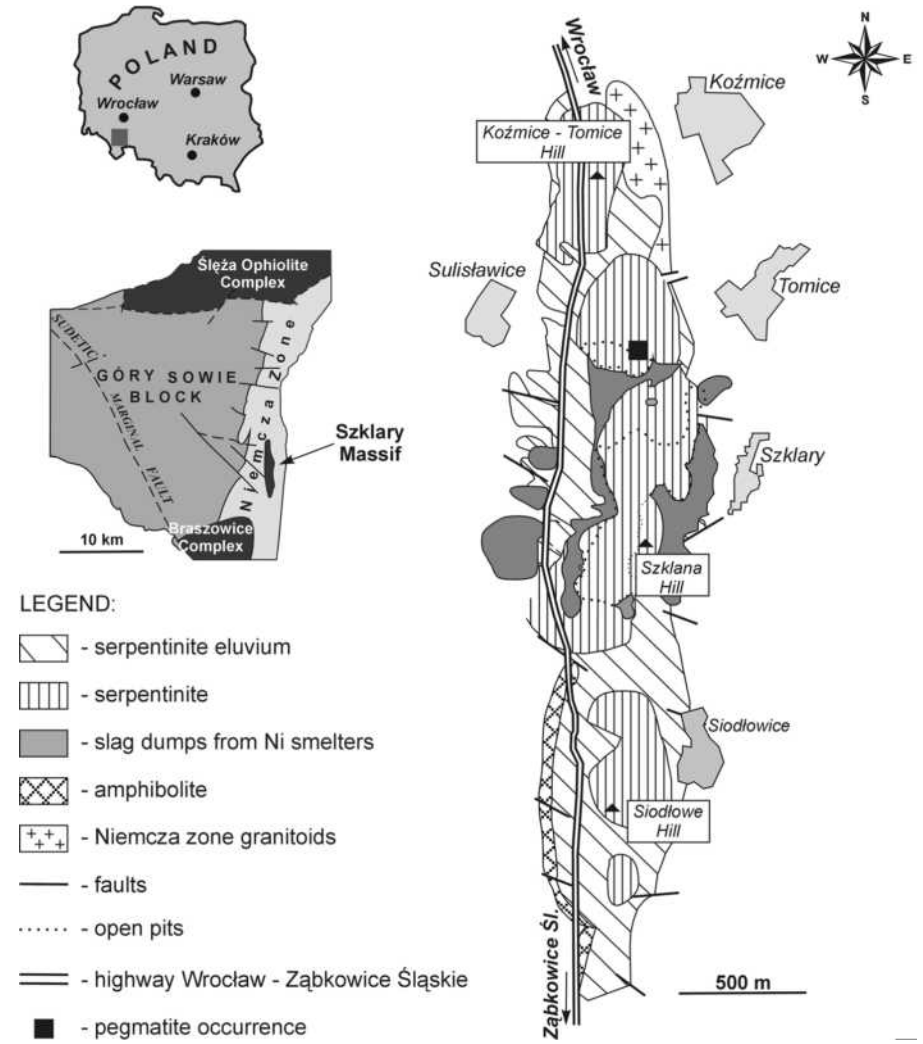

FIGURE 1. Map showing the location and geology of the Szklary serpentinite massif (after Niśkiewicz 1967; Michalik 2000).

The Szklary pegmatite is similar to pegmatites in the nearby Góry Sowie gneissic complex [374–380 Ma (van Breemen et al. 1988; Timmermann et al. 2000)] with respect to mode of occurrence, internal structure, mineral composition, and age of formation (ca. 390 Ma), however, the origin of the pegmatite is not clear. The presence of cordierite in the border zone and chrysoberyl in the inner zone suggests that the pegmatite has been affected by a metamorphic overprint. Metamorphism of pelitic-psammitic sediments in the Góry Sowie complex, reached upper amphibolite facies and led to widespread migmatization and metamorphic segregation. Intrusion of granitic magma during uplift of the Góry Sowie complex ca. 370–380 Ma led to the formation of dikes and veins of pegmatite with abundant black tourmaline, ranging in composition from the muscovite (MS) to the rare element (REL) class (Černý and Ercit, 2005). The Szklary dike is probably related to these pegmatites and represents a body, intruded into the rocks surrounding the Góry Sowie complex.

Prior to 2002, the pegmatite was very poorly exposed, but its general mineral content and zoned nature was known (Pieczka 2000). In the autumn of 2002, mineral collectors excavated the dike and removed much of the material so that samples collected for study here are not located with respect to a specific zone. Field observations show that the dike is in contact with a white aplite to the northwest and an amphibolite to the southeast. Both contact rocks are strongly altered to clay-rich and talc + chlorite + vermiculite assemblages.

The pegmatite dike is zoned, consisting of a border zone composed of graphic intergrowths of albite and quartz, aggregates of biotite altered to clinochlore, and black tourmaline. Inward from the border zone, perthitic microcline gradually replaces albite, and the pegmatite grades to a coarsely crystalline, biotite-free inner zone with more common muscovite and tourmaline. The axial part of the inner zone consists of graphic intergrowths of microcline and quartz, with occasional nests of black tourmaline. A quartz core is absent.

Dike feldspar-group minerals are commonly enriched in phosphorus (0.5–0.6 wt% P_2O_5). Potassium-feldspars contain 0.13–0.20 wt% Rb, and their K/Rb mass ratio ranges from about 90 to 60. Tourmaline is commonly represented by dark, Fe^{3+}-

bearing, Li-free intermediate members of the schorl-dravite series (Pieczka and Kraczka 1996), or less frequently, by blue dravite representing a transitional member among the dravite, schorl, and olenite end-members (Pieczka 2007b). With the exception of the major rock-forming minerals, tourmaline, spessartine, chrysoberyl, apatite, and beusite-oxide aggregates, the remaining constituents within the dike occur as small grains not exceeding a few millimeters in size.

The primary Nb- and Ta-bearing minerals investigated herein were found exclusively within samples derived from the inner zone of the pegmatite, commonly in association with black tourmaline, spessartine, beusite, Mn-rich fluorapatite, hydroxylapatite, or chlorapatite, and aggregates of Mn-oxides. Chrysoberyl, fersmite, zircon, cheralite, xenotime-(Y), uraninite, native antimony, arsenic, bismuth, and gold, paradocrasite, stibarsen, pollucite, natrophyllite, purpurite, alluaudite, gorceixite, plumbogummite, phosphohedyphane, mitridatite, unnamed Mn-dominant apatite-like phase $Mn_3Ca_2(PO_4)_3Cl$, Ba- and Pb-dominant members of the dickinsonite group, $MnAs_2O_4$, $Al_4As_2O_9$, $Mn_3UAs_2Sb_2Ta_2Ti_2O_{20}$, and various pyrochlore-group minerals also occur in the inner zone.

TABLE 1. Conditions of EMP analyses

Element	Standard	Analytical line	Crystal	Detection limit (wt%)	σ (wt%)
F	phlogophite	*K*α	TAP	0.04–0.05	0.12–0.14
Na	albite	*K*α	TAP	0.02–0.03	0.01–0.02
Mg	diopside	*K*α	TAP	0.02	0.01
Al	orthoclase	*K*α	TAP	0.02	0.08
Si	diopside	*K*α	TAP	0.02–0.06	0.02–0.04
P	apatite	*K*α	PET	0.03	0.01
K	orthoclase	*K*α	PET	0.03	0.01
Ca	diopside	*K*α	PET	0.02–0.04	0.01–0.03
Sc	pure Sc	*K*α	PET	0.02–0.03	0.01–0.02
Ti	rutile	*K*α	LIF	0.07–0.10	0.04–0.13
Mn	rhodonite	*K*α	LIF	0.06–0.09	0.03–0.14
Fe	hematite	*K*α	LIF	0.06–0.09	0.03–0.10
As	GaAs	*L*α	TAP	0.04–0.07	0.03–0.08
Zr	zircon	*L*α	PET	0.09–0.12	0.04–0.08
Nb	pure Nb	*L*α	PET	0.10–0.15	0.05–0.35
Sn	cassiterite	*L*α	PET	0.08–0.12	0.03
Sb	InSb	*L*α	PET	0.06–0.10	0.07–0.26
Ba	barite	*L*β	PET	0.17–0.19	0.08–0.10
Ta	pure Ta	*M*α	TAP	0.06–0.09	0.04–0.17
W	scheelite	*M*α	PET	0.11–0.16	0.05–0.08
Pb	galena	*M*α	PET	0.14–0.20	0.08–0.27
Bi	Bi_2Te_3	*M*α	PET	0.11–0.18	0.05–0.35
U	UO_2	*M*β	PET	0.13–0.16	0.04–0.23
Th	ThO_2	*M*α	PET	0.14–0.26	0.04–0.08

ANALYTICAL METHODS

Electron microprobe analyses (EMPA) were performed at the Inter-Institute Analytical Complex for Minerals and Synthetic Substances of the University of Warsaw with a CAMECA SX-100 electron microprobe operating in wavelength dispersive (WDS) mode. Operating conditions include an accelerating voltage of 20 kV, beam current of 15 nA, beam diameter around 2 µm, peak count time 20 s, and background time 10 s. Table 1 presents standards, analytical lines, diffracting crystals, detection limits, and 1σ errors for analyzed elements. Data were corrected with the PAP procedure (Pouchou and Pichoir 1985). Because the radius of $^{[6]}As^{3+}$ is only 0.58 Å (Shannon 1976), this atypical component of the Nb-Ta minerals has been included in the mineral formulae together with Nb, and other small cations, except for the unnamed (As,Sb,U)-rich (Ta,Ti)-oxide and holtite, where As^{3+} substitutes for Sb^{3+}. The formulae of columbite-group minerals (CGM) have been normalized to 6 O atoms per formula unit (apfu), those of stibiocolumbite and stibiotantalite to 4 O apfu, and that of holtite to an amount of oxygen equal to ($18-N_{As}-N_{Sb}$) apfu, where N_{As} and N_{Sb} denote the amounts of As and Sb in the formula.

The formulae of alteration products, fersmite and pyrochlore-group minerals (PGM), have not been calculated, due to the common presence of high to very high amounts of silicon. Although the role of Si in PGM is still unclear, Bonazzi et al. (2006) showed that only about 30–50% of the Si detected by EMPA is incorporated in the B site, whereas the remaining 50–70% is incorporated in the radiation-damaged portion of the structure. It is also possible that Si is only a mechanical admixture of nanoparticles undetectable in back-scattered electron (BSE) images, or with other conventional imaging techniques; e.g., Chakhmouradian and Mitchell (2002), suggested that it could represent submicroscopic intergrowths of pyrochlore with an Nb-bearing silicate.

MINERALOGY OF THE PRIMARY Nb-Ta MINERALS IN THE SZKLARY PEGMATITE

Columbite-group minerals

Columbite-group minerals occur in the Szklary pegmatite as discrete, commonly thin, elongate (to 10 mm) crystals disseminated within quartz and potassium-feldspars in the inner zone. They are also found within chrysoberyl, schorl-dravite intermediate members, spessartine, Mn-rich fluorapatite, and in aggregates of Mn-bearing oxides. The crystals are typically poorly zoned, with a core corresponding to columbite-(Mn), and a thin rim of Ta-bearing columbite-(Mn) or tantalite-(Mn) (Fig. 2a). More complex compositional zoning patterns, with a few intermediate zones, are developed in some crystals of the CGM (Figs. 2b–2f). These crystals, representing both columbite-(Fe) and columbite-(Mn), sometimes show a patchy texture (Figs. 2c and 2d). Crystals of the CGM are replaced by fersmite (Figs. 2d and 2g), and less commonly by pyrochlore, bismutopyrochlore, and Bi-bearing plumbopyrochlore (Figs. 2d, 2f, and 2h) or members of the stibiocolumbite-stibiotantalite series. Bismutopyrochlore and plumbopyrochlore form deeply penetrating veinlets within columbite-(Fe) or columbite-(Mn) (Figs. 2d and 2f), or are present as small patches within these minerals or within pyrochlore that replaces the CGM (Figs. 2d and 2h).

The CGM from the Szklary pegmatite (Tables 2a–2c[1], 3a–3b[1], and 4a–4b[1]) show three different compositional trends summarized in Figure 3. The most commonly observed trend I initially involves Mn-Fe and Ta-Nb fractionation typical of CGM from rare-element pegmatites, which is followed by a sharp increase in Ta content at progressively increasing Mn/(Mn+Fe) ratio. The Ta-enrichment peak [at Ta/(Ta+Nb) ~0.60] in crystals of columbite-(Mn) evolving toward tantalite-(Mn) occurs at a Mn/(Mn+Fe) ratio ranging from 0.85 to 0.87. With further Mn-Fe fractionation, the Ta content first decreases, and then, at Mn/(Mn+Fe) values above 0.92, increases slightly. This increase may indicate that the pegmatite-forming melt reached a stage in Mn-Fe fractionation typical of Li-bearing pegmatites (e.g., those of the lepidolite subtype). Compositional trend II initially involves an increase in the Ta/(Ta+Fe) ratio with decreasing Mn/(Mn+Fe) ratio followed by a nearly constant Mn/(Mn+Fe) ratio as the Ta/(Ta+Nb) ratio increases to reach a value of ca. 0.60. Such crystals of columbite-(Mn) have Mn/(Mn+Fe) = 0.78 in the cores to 0.70–0.72 in the rims. Trend III relates to the crystallization of columbite-(Fe) and columbite-(Mn). It initially shows a slight increase in Ta/(Ta+Nb) ratio from 0.10 to 0.16 at

[1] Deposit item AM-10-052, Tables 2b, 2c, 3b, and 4b). Deposit items are available two ways: For a paper copy contact the Business Office of the Mineralogical Society of America (see inside front cover of recent issue) for price information. For an electronic copy visit the MSA web site at http://www.minsocam.org, go to the *American Mineralogist* Contents, find the table of contents for the specific volume/issue wanted, and then click on the deposit link there.

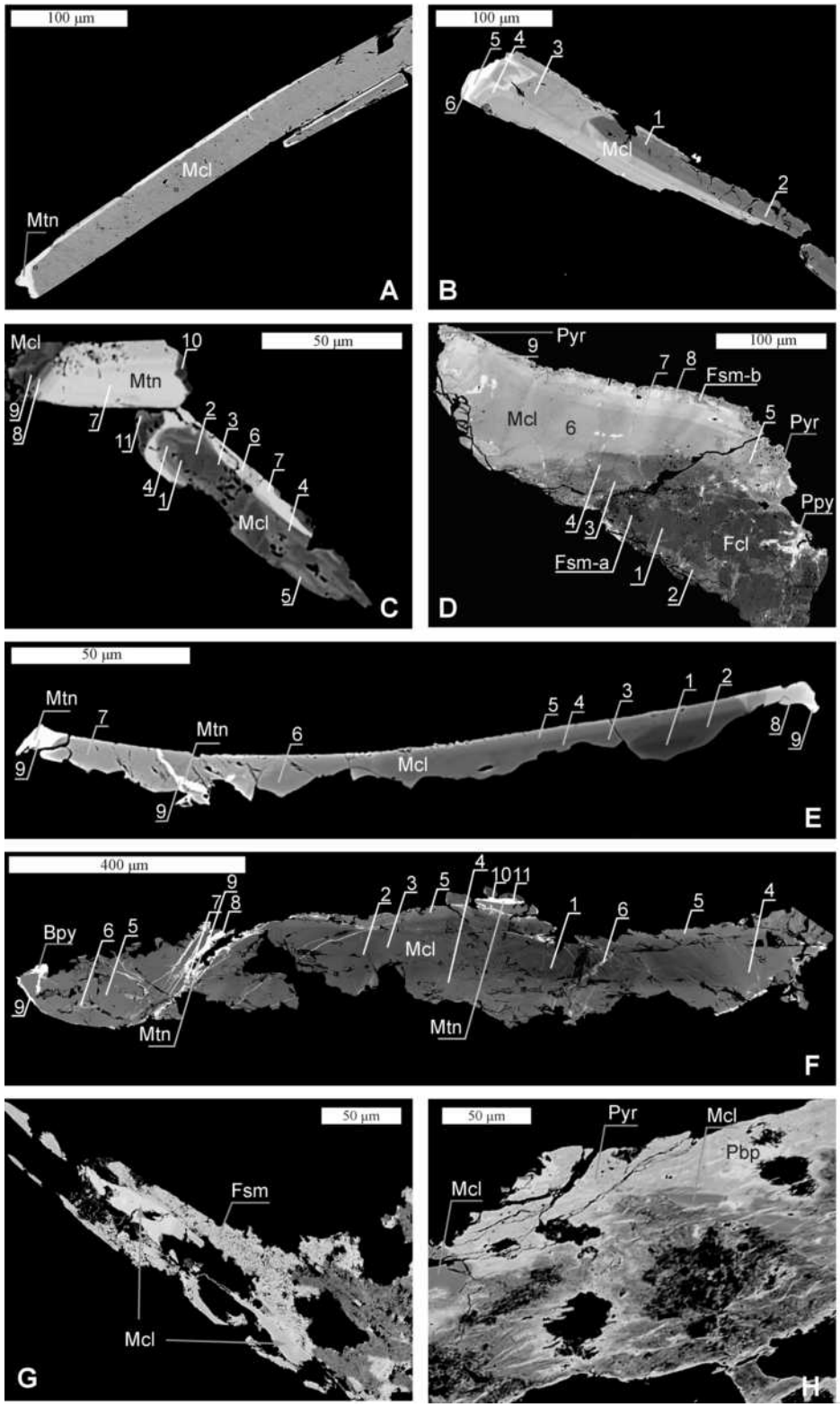

Figure 2. Representative BSE images of CGM from the Szklary pegmatite: (**a**) typical zoning pattern in columbite-(Mn) (Sz1); (**b**) regularly zoned crystal of columbite-(Mn) (Sz5); (**c**) crystal of patchy-zoned columbite-(Mn) grading outward to Ta-bearing columbite-(Mn) (Sz3); (**d**) crystal of patchy-zoned columbite-(Fe) overgrown by columbite-(Mn) altered to fersmite and PGM (Sz11); (**e**–**f**) crystals of columbite-(Mn) grading into tantalite-(Mn) (Mp3 and Sz18); (**g**) fersmite overgrowths on relict grains of columbite-(Mn) (SzA); (**h**) pyrochlore containing relics of a crystal of columbite-(Mn) (Sz2). Sample numbers are given in parentheses. Numbers in the images correspond to the chemical analyses in Tables 2–4. Abbreviations: Fcl = columbite-(Fe), Mcl = columbite-(Mn), Mtn = tantalite-(Mn), Fsm = fersmite, Pyr = pyrochlore, Ppy = plumbopyrochlore, Bpy = bismutopyrochlore, Pbp = Pb-rich bismutopyrochlore.

TABLE 2a. Representative compositions of columbite-group minerals from the Szklary pegmatite, Mn-Fe, Ta-Nb fractionation trend I

Sz3	1	2	3	4	5	6	7	8	9	10	11
						wt%					
WO_3	2.80	1.75	1.26	1.26	1.93	1.62	1.67	2.26	1.09	2.03	1.58
Nb_2O_5	69.24	68.79	67.14	65.30	60.78	58.01	41.46	63.80	73.47	68.41	66.27
Ta_2O_5	6.22	8.34	10.85	12.52	16.15	19.72	38.08	12.79	4.27	8.64	11.97
TiO_2	1.31	0.93	0.54	0.67	1.07	0.77	0.99	1.09	0.64	0.61	0.49
ZrO_2	0.00	0.00	0.00	0.00	0.00	0.00	0.00	0.00	0.00	0.00	0.00
SnO_2	0.00	0.00	0.00	0.00	0.00	0.00	0.00	0.00	0.00	0.00	0.00
UO_2	0.20	0.00	0.00	0.13	0.20	0.00	0.17	0.26	0.00	0.00	0.00
Sc_2O_3	0.05	0.03	0.02	0.03	0.08	0.05	0.10	0.08	0.06	0.05	0.05
FeO	3.10	3.86	4.37	4.13	3.52	3.11	2.48	2.68	1.91	1.38	0.99
MnO	16.97	16.09	15.48	15.52	15.62	15.85	15.13	17.02	18.78	18.71	18.94
MgO	0.07	0.11	0.13	0.10	0.08	0.09	0.05	0.04	0.00	0.01	0.02
CaO	0.00	0.00	0.00	0.00	0.00	0.00	0.00	0.00	0.00	0.00	0.00
Total	99.97	99.90	99.78	99.66	99.44	99.23	100.11	100.03	100.22	99.85	100.31
						Atomic contents based on O = 6 apfu					
Fe^{2+}	0.150	0.188	0.215	0.205	0.178	0.160	0.137	0.133	0.091	0.067	0.049
Mn^{2+}	0.831	0.792	0.771	0.780	0.800	0.825	0.848	0.855	0.906	0.925	0.944
Mg^{2+}	0.006	0.010	0.011	0.009	0.007	0.008	0.005	0.004	0.000	0.001	0.002
Ca^{2+}	0.000	0.000	0.000	0.000	0.000	0.000	0.000	0.000	0.000	0.000	0.000
Sc^{3+}	0.003	0.001	0.001	0.002	0.004	0.003	0.006	0.004	0.003	0.002	0.002
U^{4+}	0.003	0.000	0.000	0.002	0.003	0.000	0.002	0.003	0.000	0.000	0.000
ΣA site	0.992	0.991	0.998	0.997	0.992	0.996	0.998	1.000	1.000	0.996	0.997
W^{6+}	0.042	0.026	0.019	0.019	0.030	0.026	0.029	0.035	0.016	0.031	0.024
Nb^{5+}	1.808	1.807	1.785	1.751	1.661	1.612	1.240	1.711	1.892	1.805	1.763
Ta^{5+}	0.098	0.132	0.174	0.202	0.265	0.330	0.685	0.206	0.066	0.137	0.191
Ti^{4+}	0.057	0.041	0.024	0.030	0.049	0.036	0.049	0.048	0.027	0.027	0.022
Zr^{4+}	0.000	0.000	0.000	0.000	0.000	0.000	0.000	0.000	0.000	0.000	0.000
Sn^{4+}	0.000	0.000	0.000	0.000	0.000	0.000	0.000	0.000	0.000	0.000	0.000
ΣB site	2.005	2.006	2.002	2.002	2.005	2.003	2.003	2.000	2.002	2.000	2.000
O^{2-}	6	6	6	6	6	6	6	6	6	6	6
Mn/(Mn+Fe)	0.847	0.808	0.782	0.792	0.818	0.838	0.861	0.866	0.909	0.932	0.951
Ta/(Ta+Nb)	0.051	0.068	0.089	0.103	0.138	0.170	0.356	0.108	0.034	0.071	0.098

Note: 0.00 wt% = a content below the respective detection limit.

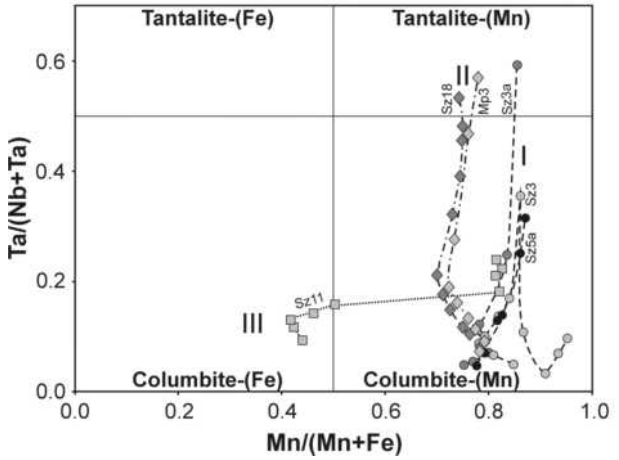

FIGURE 3. Mn-Fe and Ta-Nb fractionation trends (core to rim) in individual crystals of the Szklary CGM in the quadrilateral plot Ta/(Ta+Nb) vs. Mn/(Mn+Fe). The three principal compositional trends exhibited by the CGM are shown by the dashed line (trend I), dotted-dashed line (trend II), and dotted line (trend III). Sz3, Sz3a, Sz5a, Sz11, Sz18, and Mp3 correspond to sample numbers.

variable Mn/(Mn+Fe) values fluctuating from 0.42 to 0.50. This is followed by growth of a zoned columbite-(Mn) that crystallized after a compositional gap at much higher, but almost constant Mn/(Mn+Fe) ratio, ~0.81–0.82, and with increasing Ta/(Ta+Nb) ratio from 0.18 to 0.24.

All columbite-(Mn) that exhibit evolution toward tantalite-(Mn) is poor in Mg (usually below 0.15 wt% MgO), however, columbite-(Fe) is clearly enriched in this element, up to 1.39 wt% MgO in Sz1 (Table 3b[1]). As a result, Mg shows a distinct negative correlation with respect to Mn/(Mn+Fe) (Fig. 4a). The Sc content progressively increases with Ta/(Nb+Ta) ratio, reaching a maximum of 0.3 wt% Sc_2O_3 (~0.02 Sc apfu) in the rim of Ta-bearing columbite-(Mn) evolving to tantalite-(Mn). In columbite-(Fe), the Sc content is lower (Fig. 4b).

Uranium, which is uncommon in CGM, is generally less than 0.2 wt% UO_2 in the Szklary samples. However, in internal zones of some crystals, the UO_2 content reaches to 1.3 wt% (Table 3a). Tungsten and Ti are the main substituents for Nb and Ta. The content of W, reaching a maximum of about 3.5 wt% WO_3 in internal zones, decreases toward the rim of some crystals. Titanium is commonly present in concentrations ranging from 0.6 to 2.0 wt% TiO_2 in columbite-(Mn) and tantalite-(Mn), but in columbite-(Fe), the TiO_2 content attains over 3.0 wt%. Zirconium is usually present in concentrations comparable to the detection limit of WDS, but some crystals of CGM contain up to 0.40 wt% ZrO_2 (Table 3a). Tin is not present in detectable concentrations in the CGM from Szklary.

Stibiocolumbite-group minerals (SCGM)

Bright yellow to gray-green stibiocolumbite, $Sb(Nb,Ta)O_4$, is found as a replacement and overgrowth mineral on large grains of columbite-(Mn) (Figs. 5a–5c). Stibiocolumbite is also common among fibers of holtite. Stibiotantalite, $Sb(Ta,Nb)O_4$, occurring as discrete crystals up to 0.5 mm in diameter (Fig. 5d), is rare at Szklary. This mineral is sometimes found as inclusions in the PGM (Figs. 5e–5f), but was not observed as intergrowths with the CGM. Stibiocolumbite is replaced along fractures by Bi-rich pyrochlore (Fig. 5b) or is overgrown by Bi-dominant betafite (Fig. 5g), whereas stibiotantalite is replaced by bismutomicrolite

TABLE 3a. Representative compositions of columbite-group minerals from the Szklary pegmatite, Mn-Fe, Ta-Nb fractionation trend II

Mp3	1	2	3	4	5	6	7	8	9
					wt%				
WO_3	2.27	1.94	2.73	2.20	2.42	1.70	2.55	2.21	2.10
Nb_2O_5	67.14	64.89	62.63	60.81	57.13	54.86	45.31	31.48	24.59
Ta_2O_5	8.75	10.95	13.27	15.69	18.39	21.59	28.89	46.27	54.07
TiO_2	1.34	1.46	1.37	1.45	1.79	2.33	3.28	2.16	1.66
ZrO_2	0.11	0.13	0.18	0.15	0.14	0.20	0.40	0.22	0.22
SnO_2	0.00	0.00	0.00	0.00	0.00	0.00	0.00	0.00	0.00
UO_2	0.00	0.00	0.26	0.18	0.16	0.15	1.29	0.20	0.41
Sc_2O_3	0.03	0.05	0.05	0.10	0.11	0.17	0.22	0.15	0.13
FeO	4.43	4.22	4.49	4.65	5.02	5.37	4.85	4.16	3.56
MnO	15.65	15.68	15.11	14.57	14.03	13.77	13.07	12.79	12.30
MgO	0.10	0.07	0.11	0.14	0.14	0.12	0.09	0.08	0.13
CaO	0.00	0.00	0.00	0.00	0.00	0.00	0.00	0.00	0.00
Total	99.82	99.39	100.21	99.95	99.32	100.27	99.94	99.71	99.17
					Atomic contents based on O = 6 apfu				
Fe^{2+}	0.216	0.209	0.223	0.233	0.256	0.274	0.258	0.240	0.215
Mn^{2+}	0.773	0.784	0.760	0.740	0.725	0.712	0.705	0.748	0.755
Mg^{2+}	0.009	0.007	0.009	0.012	0.013	0.011	0.009	0.008	0.014
Ca^{2+}	0.000	0.000	0.000	0.000	0.000	0.000	0.000	0.000	0.000
Sc^{3+}	0.002	0.003	0.003	0.005	0.006	0.009	0.012	0.009	0.008
U^{4+}	0.000	0.000	0.003	0.002	0.002	0.002	0.018	0.003	0.007
ΣA site	1.000	1.002	0.998	0.994	1.002	1.007	1.002	1.008	0.999
W^{6+}	0.034	0.030	0.042	0.034	0.038	0.027	0.042	0.039	0.039
Nb^{5+}	1.770	1.733	1.681	1.848	1.577	1.513	1.304	0.982	0.805
Ta^{5+}	0.139	0.176	0.214	0.256	0.305	0.358	0.500	0.869	1.065
Ti^{4+}	0.059	0.065	0.061	0.065	0.082	0.107	0.157	0.112	0.091
Zr^{4+}	0.003	0.004	0.005	0.004	0.004	0.006	0.012	0.007	0.008
Sn^{4+}	0.000	0.000	0.000	0.000	0.000	0.000	0.000	0.000	0.000
ΣB site	2.005	2.006	2.004	2.008	2.007	2.012	2.015	2.010	2.008
O^{2-}	6	6	6	6	6	6	6	6	6
Mn/(Mn+Fe)	0.782	0.790	0.773	0.760	0.739	0.722	0.732	0.757	0.778
Ta/(Ta+Nb)	0.073	0.092	0.113	0.134	0.162	0.191	0.277	0.469	0.569

Note: 0.00 wt% = a content below the respective detection limit.

TABLE 4a. Representative compositions of columbite-group minerals from the Szklary pegmatite, Mn-Fe, Ta-Nb fractionation trend III

Sz11	1	2	3	4	5	6	7	8	9
					wt%				
WO_3	3.82	3.00	3.81	3.34	1.43	1.80	1.59	1.80	2.08
Nb_2O_5	62.16	60.39	58.50	58.00	58.78	56.73	53.69	52.64	50.31
Ta_2O_5	10.82	13.56	14.66	16.03	18.52	20.93	23.86	25.17	26.48
TiO_2	3.22	2.77	3.25	2.68	1.86	1.41	1.42	1.43	1.52
ZrO_2	0.00	0.00	0.00	0.00	0.00	0.00	0.00	0.00	0.00
SnO_2	0.00	0.00	0.00	0.00	0.00	0.00	0.00	0.00	0.00
UO_2	0.00	0.00	0.00	0.00	0.00	0.18	0.22	0.25	0.18
Sc_2O_3	0.05	0.08	0.09	0.08	0.18	0.14	0.17	0.15	0.17
FeO	11.07	11.07	11.32	10.35	9.11	3.48	3.56	3.32	3.44
MnO	8.47	7.98	7.94	8.65	9.04	15.60	15.18	15.41	14.88
MgO	0.52	0.51	0.51	0.44	0.72	0.07	0.07	0.06	0.08
CaO	0.00	0.00	0.00	0.00	0.13	0.00	0.00	0.00	0.00
Total	100.12	99.38	100.07	99.57	99.78	100.35	99.77	100.23	99.14
					Atomic contents based on O = 6 apfu				
Fe^{2+}	0.541	0.551	0.562	0.520	0.459	0.178	0.185	0.173	0.182
Mn^{2+}	0.419	0.402	0.400	0.441	0.461	0.806	0.799	0.813	0.799
Mg^{2+}	0.045	0.046	0.045	0.040	0.065	0.007	0.007	0.006	0.008
Ca^{2+}	0.000	0.000	0.000	0.003	0.009	0.000	0.000	0.000	0.000
Sc^{3+}	0.002	0.004	0.005	0.004	0.010	0.007	0.009	0.008	0.009
U^{4+}	0.000	0.000	0.000	0.000	0.000	0.002	0.003	0.003	0.003
ΣA site	1.007	1.004	1.012	1.005	1.003	1.000	1.003	1.002	1.001
W^{6+}	0.058	0.046	0.059	0.052	0.022	0.028	0.026	0.029	0.034
Nb^{5+}	1.642	1.624	1.571	1.576	1.600	1.564	1.508	1.481	1.442
Ta^{5+}	0.172	0.219	0.237	0.262	0.303	0.347	0.403	0.426	0.456
Ti^{4+}	0.142	0.124	0.145	0.121	0.084	0.065	0.066	0.067	0.072
Zr^{4+}	0.000	0.000	0.000	0.000	0.000	0.000	0.000	0.000	0.000
Sn^{4+}	0.000	0.000	0.000	0.000	0.000	0.000	0.000	0.000	0.000
ΣA site	2.013	2.013	2.012	2.011	2.009	2.005	2.004	2.004	2.005
O^{2-}	6	6	6	6	6	6	6	6	6
Mn/(Mn+Fe)	0.437	0.422	0.415	0.459	0.501	0.819	0.812	0.825	0.814
Ta/(Ta+Nb)	0.095	0.119	0.131	0.143	0.159	0.182	0.211	0.223	0.240

Note: 0.00 wt% = a content below the respective detection limit.

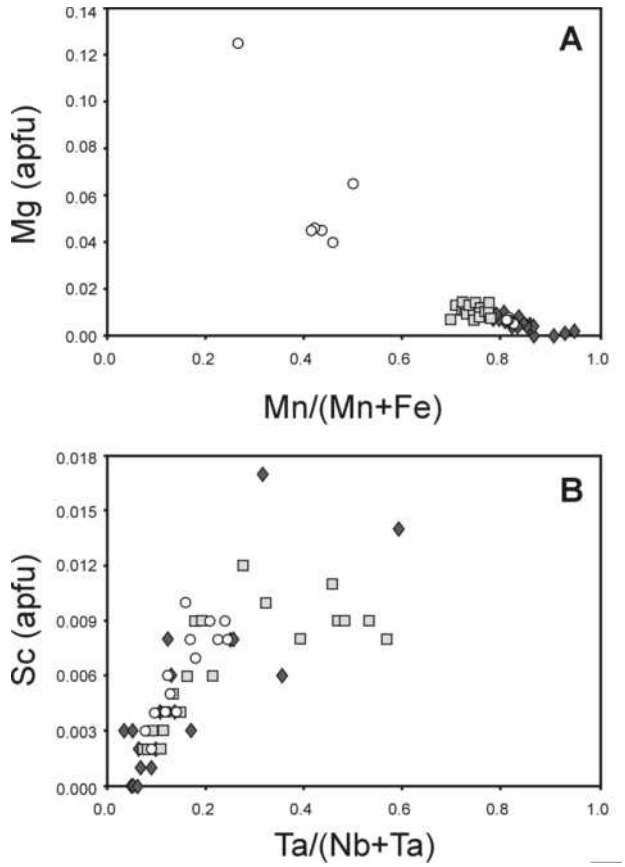

FIGURE 4. Compositional variation of the CGM from Szklary: (**a**) Mg (apfu) vs. Mn/(Mn+Fe); (**b**) Sc (apfu) vs. Ta/(Ta+Nb). Diamonds and squares denote columbite-(Mn) grading into tantalite-(Mn) according to trends I and II, respectively; circles denote columbite-(Fe) grading into columbite-(Mn) according to trend III.

(Fig. 5d) or stibiomicrolite, uranmicrolite, and betafite (Figs. 5d–5e). Native antimony, bismuth, paradocrasite, and, more rarely, arsenic are typical fine-grained inclusions in feldspars bordering stibiocolumbite and stibiotantalite.

Antimony, Nb, and Ta are the main components in the SCGM; W, Bi, As, and Ti are subordinate components, whereas other elements such as Mn and Pb, are commonly below detection limits of WDS (Table 5). Tungsten and Ti are usually present at levels below 2.0 wt% WO_3 and 1.0 wt% TiO_2, respectively, i.e., lower than their concentrations in the coexisting columbite-(Mn). Arsenic is commonly present in concentrations of about 0.7–0.8 wt% As_2O_3. The Bi content is variable, but rather low, ranging from 0.14 wt% Bi_2O_3 in discrete crystals of stibiotantalite replaced by bismutomicrolite, to 4.7 wt% Bi_2O_3 in relics of stibiotantalite replaced by stibiomicrolite, uranmicrolite, and betafite, and up to 6.5 wt% Bi_2O_3 in stibiocolumbite coexisting with columbite-(Mn) and fersmite.

In stibiocolumbite that replaces the CGM, the Bi/(Bi+Sb) ratio, reflecting Bi-Sb fractionation, is commonly low and does not exceed 0.04, except for the stibiocolumbite coexisting with columbite-(Mn) and fersmite (Fig. 2g), in which that ratio reaches 0.08. Moderate values of Bi/(Bi+Sb), but lower than 0.04, are also

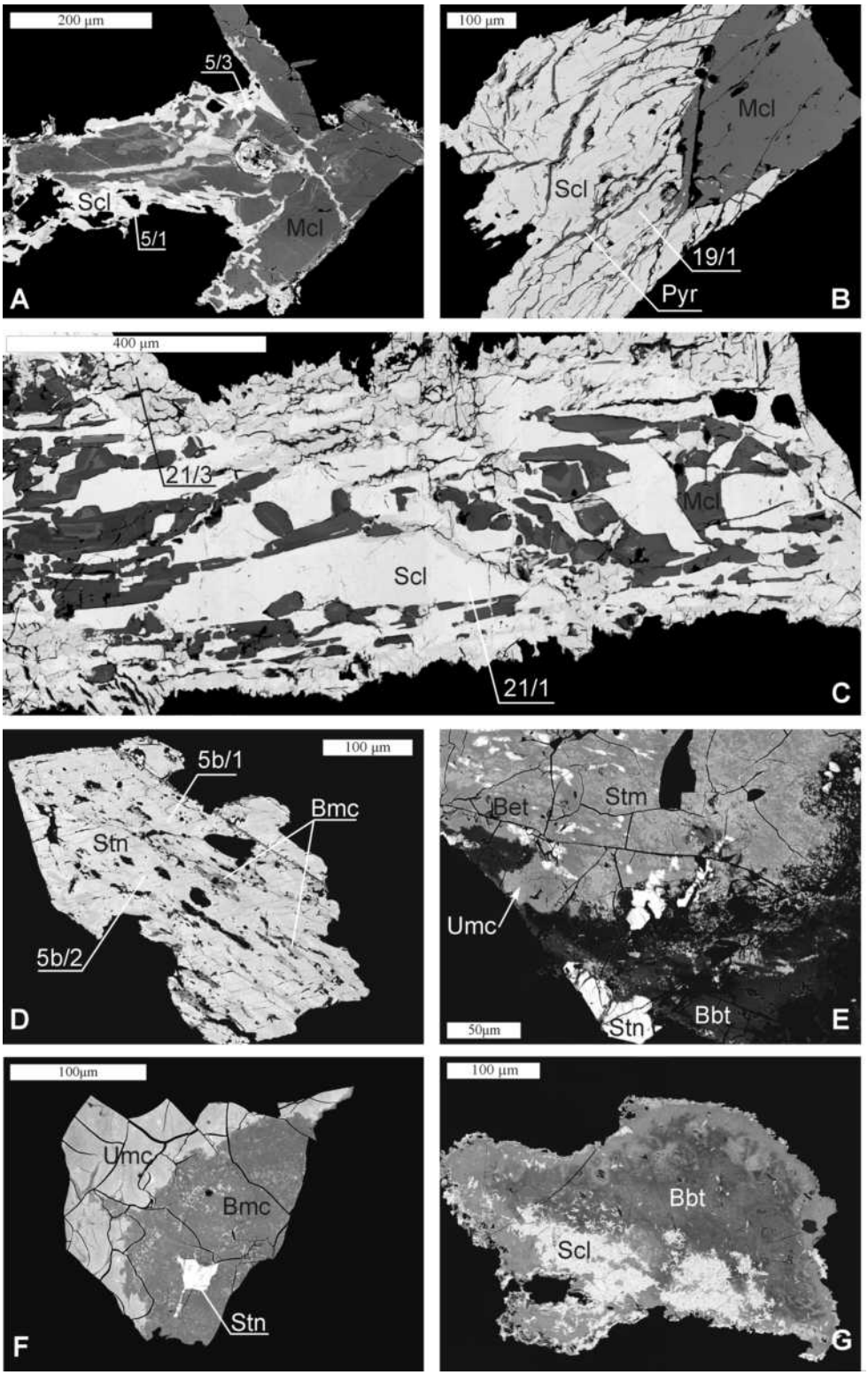

Figure 5. Representative BSE images of stibiocolumbite and stibiotantalite from the Szklary pegmatite: (**a**) columbite-(Mn) altered to stibiocolumbite (Sz5); (**b**) columbite-(Mn) overgrown by poorly zoned stibiocolumbite (Sz19); (**c**) stibiocolumbite (Sz21) replacing columbite-(Mn); (**d**) stibiotantalite partly altered to bismutomicrolite (Sz5a); (**e**) stibiotantalite altered to stibiomicrolite, uranmicrolite, betafite, and Bi-dominant betafite (Sz18); (**f**) stibiotantalite altered to uranmicrolite and bismutomicrolite (Sz13); (**g**) stibiocolumbite overgrown by Bi-dominant betafite (Sz27). Sample numbers are given in parentheses. Numbers in the BSE images correspond to the analyses in Table 5. Abbreviations: Mcl = columbite-(Mn), Scl = stibiocolumbite, Stn = stibiotantalite, Pyr = pyrochlore, Bmc = bismutomicrolite, Umc = uranmicrolite, Stm = stibiomicrolite, Bet = betafite, Bbt = Bi-dominant betafite.

TABLE 5. Representative compositions of stibiocolumbite and stiobiotantalite from the Szklary pegmatite

	SzA*	Sz5/1*	Sz5/3*	Sz19/1*	Sz19/3*	Sz21/1*	Sz21/3*	Sz24	Sz27	Sz30/1*	Sz30/2*	Sz35†	Sz5b/1	Sz5b/2	Sz13/3	Sz13/4	Sz18/1	Sz18/3
									wt%									
WO_3	2.09	1.41	1.36	1.76	1.94	1.86	0.95	0.38	1.10	2.01	3.19	2.64	1.14	0.69	3.95	2.31	0.76	1.32
Nb_2O_5	38.43	39.16	27.14	40.67	36.92	31.48	38.36	21.09	26.63	35.43	31.95	33.08	15.93	14.27	14.64	9.72	14.65	6.92
Ta_2O_5	6.23	6.18	21.51	4.42	8.69	15.17	8.20	29.81	22.42	11.01	13.88	11.82	37.87	40.01	34.57	43.49	37.08	46.89
TiO_2	0.75	0.86	1.17	0.57	0.74	1.29	0.71	0.99	0.44	0.93	1.08	1.26	0.24	0.27	1.61	0.92	0.80	0.80
As_2O_3	0.54	0.77	0.71	0.72	0.84	0.79	0.84	0.70	0.74	0.85	0.83	0.75	0.67	0.66	0.59	0.57	0.79	0.66
Sb_2O_3	45.56	50.16	45.55	49.82	47.65	48.22	49.79	44.15	43.70	49.45	48.45	46.78	43.33	43.97	44.20	42.57	40.45	39.29
Bi_2O_3	6.46	0.50	2.63	1.32	2.34	1.13	0.72	2.48	2.72	0.31	0.73	2.95	0.19	0.14	0.80	0.44	4.66	3.67
MnO	0.00	0.09	0.00	0.00	0.00	0.00	0.00	0.00	0.00	0.00	0.00	0.00	0.00	0.00	0.00	0.00	0.00	0.00
PbO	0.19	0.00	0.00	0.00	0.00	0.00	0.00	0.00	0.97	0.00	0.00	0.00	0.00	0.00	0.00	0.00	0.00	0.00
Total	100.26	99.13	100.06	99.27	99.12	99.93	99.57	99.61	98.73	99.99	100.12	99.27	100.38	100.00	100.36	100.03	99.19	99.55
									Atomic contents based on O = 4 apfu									
Sb^{3+}	0.921	0.999	0.964	0.988	0.966	0.992	0.995	0.974	0.950	0.996	0.991	0.963	1.001	1.006	0.989	0.993	0.939	0.950
Bi^{3+}	0.082	0.006	0.035	0.016	0.030	0.015	0.009	0.034	0.037	0.004	0.009	0.038	0.003	0.002	0.011	0.006	0.068	0.055
Mn^{2+}	0.000	0.004	0.000	0.000	0.000	0.000	0.000	0.000	0.000	0.000	0.000	0.000	0.000	0.000	0.000	0.000	0.000	0.000
Pb^{2+}	0.002	0.000	0.000	0.000	0.000	0.000	0.000	0.000	0.014	0.000	0.000	0.000	0.000	0.000	0.000	0.000	0.000	0.000
ΣA site	1.004	1.009	0.999	1.005	0.996	1.006	1.004	1.008	1.001	0.999	1.001	1.001	1.003	1.008	1.000	0.999	1.006	1.005
W^{6+}	0.027	0.018	0.018	0.022	0.025	0.024	0.012	0.005	0.015	0.025	0.041	0.034	0.016	0.010	0.056	0.034	0.011	0.020
Ta^{5+}	0.083	0.081	0.300	0.058	0.116	0.206	0.108	0.433	0.321	0.146	0.187	0.160	0.563	0.603	0.510	0.668	0.567	0.747
Nb^{5+}	0.851	0.855	0.630	0.884	0.820	0.709	0.840	0.510	0.634	0.781	0.716	0.746	0.394	0.358	0.359	0.248	0.373	0.183
Ti^{4+}	0.028	0.031	0.045	0.021	0.027	0.048	0.026	0.040	0.018	0.034	0.040	0.047	0.010	0.011	0.066	0.039	0.034	0.035
As^{3+}	0.016	0.022	0.022	0.021	0.025	0.024	0.025	0.023	0.024	0.025	0.025	0.023	0.022	0.022	0.020	0.020	0.027	0.024
ΣB site	1.005	1.007	1.015	1.005	1.013	1.011	1.009	1.011	1.012	1.012	1.009	1.011	1.006	1.004	1.010	1.009	1.011	1.009
O^{2-}	4	4	4	4	4	4	4	4	4	4	4	4	4	4	4	4	4	4
Ta/(Nb+Ta)	0.089	0.087	0.323	0.061	0.124	0.225	0.114	0.459	0.336	0.158	0.207	0.177	0.588	0.628	0.587	0.729	0.604	0.803
Bi/(Sb+Bi)	0.081	0.006	0.035	0.016	0.030	0.014	0.009	0.034	0.037	0.004	0.009	0.038	0.003	0.002	0.011	0.006	0.067	0.055
Mn/(Mn+Fe)‡	0.902–0.944	0.775–0.908		0.730–0.800		0.840–0.881				0.729–0.750								
Ta/(Ta+Nb)‡	0.050–0.092	0.052–0.251		0.049–0.070		0.081–0.191				0.060–0.223								

Note: 0.00 wt% = a content below the respective detection limit.
* Stibiocolumbite coexisting with columbite-group minerals.
† Stibiocolumbite coexisting with holtite.
‡ The Mn/(Mn+Fe) and Ta/(Ta+Nb) ratios in the coexisting columbite-group minerals.

typical of stibiocolumbite coexisting with holtite. It seems that Bi-Sb fractionation in the SCGM does not show any correlation with Ta-Nb fractionation, but parallels the Mn-Fe fractionation trends I and III exibited by the coexisting CGM (Fig. 6).

Weak zoning in the SCGM is caused by Ta-Nb fractionation during crystallization and by later alteration. In stibiocolumbite coexisting with columbite-(Mn), the Ta/(Nb+Ta) ratio ranges from 0.06 to 0.32, and is always slightly higher than in the most Ta-rich zone in the associated columbite-(Mn). For example, in the stibiocolumbite crystal shown in Figure 5b, the Ta/(Nb+Ta) value increases from 0.06 in the area adjacent to columbite-(Mn), which has Mn/(Mn+Fe) = 0.73–0.80 and Ta/(Nb+Ta) = 0.05–0.07, to 0.13 in the outermost part of the crystal. This increase may indicate that the stibiocolumbite crystallized during an increase in Ta activity corresponding to the Ta-enrichment peak in the CGM following trend I. However, another sample of stibiocolumbite (Fig. 5c), which replaces columbite-(Mn) with Mn/(Mn+Fe) ≈ 0.86 and Ta/(Nb+Ta) = 0.08 to 0.19, has a Ta/(Nb+Ta) value close to 0.23 in unaltered areas, and about 0.11 in alteration zones developed along fractures and in the outermost parts of the aggregate. In stibiotantalite, the Ta/(Nb+Ta) ratio reaches a value of 0.80.

An unnamed (As,Sb,U)-rich (Ta,Ti)-oxide phase

This phase was found in two betafite samples as a large, regular inclusion measuring about 50 × 20 μm, and a smaller, amoeba-like inclusion 20 μm in its maximum dimension (Fig. 7). The oxide is essentially homogeneous, with a very narrow compositional range (Table 6). The main constituents include U, As, Sb, Ta (Nb), Ti, and Mn (Fe). The analytical totals (close to 100 wt%) suggest that this is an oxide phase, but not a member of the pyrochlore group. A metal-to-oxygen ratio of ca. 3:5 indicates simple stoichiometry, and possible relation to $A^{2+}B_2^{4+}O_5$-type phases, best fitted to the formula $[(Mn,Fe)_{<3}U_{>1}]_{\Sigma=4}(As_2Sb_2)_{\Sigma=4}[(Ta,Nb)_{>2}Ti_{<2}]_{\Sigma=4}O_{20}$. The Mn/(Mn+Fe) and Ta/(Ta+Nb) ratios (0.78–0.82 and 0.60–0.65, respectively) suggest crystallization of this oxide under the conditions of peak Ta-enrichment, at a slightly higher Ta activity than during the crystallization of tantalite-(Mn), and also under high As and Sb activities.

Holtite

Holtite is a very rare Sb- and Ta-bearing aluminoborosilicate known from pegmatites at only three localities worldwide. Pryce (1971) identified it in specimens collected previously from an alluvial tin deposit near Greenbushes in the southwestern part of Western Australia. Voloshin et al. (1977) described a second occurrence at Mount Vasin-Myl'k, Voron'i Tundry, Kola Peninsula, Russia. Pieczka and Marszałek (1996) reported the third occurrence in the Szklary pegmatite.

At Szklary, holtite commonly occurs as aggregates of small prismatic and acicular to asbestiform aggregates that typically occur interstitially with respect to crystals of microcline, quartz, and black tourmaline. Individual crystals may reach 1 mm in length and up to 50 μm in diameter, but are typically smaller (Figs. 8a–8c). Needles of holtite were found also in Mn-bearing oxides, and, less so in quartz. In the pegmatite, holtite is usually associated with stibiocolumbite, and inclusions of native antimony, bismuth, paradocrasite, stibarsen, and less commonly

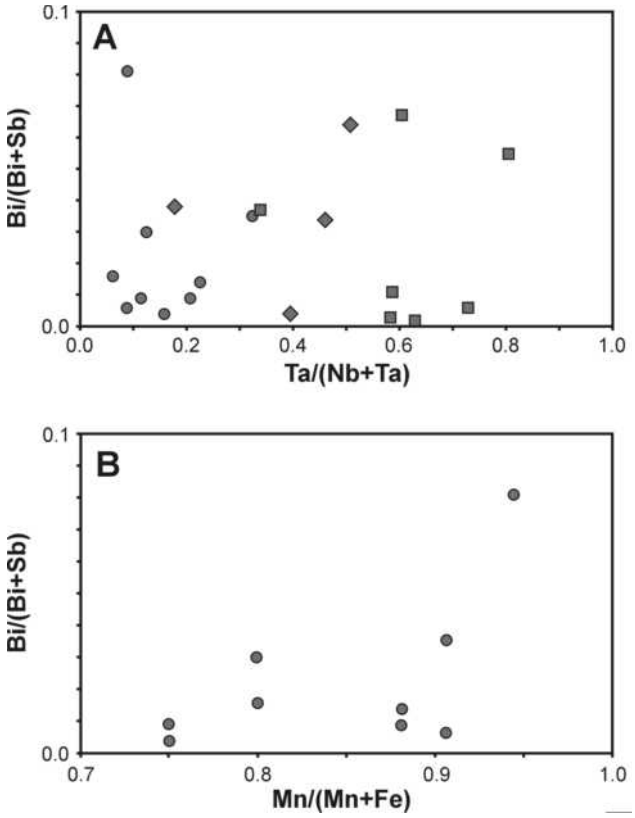

FIGURE 6. (**a**) Variation of Bi/(Bi+Sb) vs. Ta/(Ta+Nb) in stibiocolumbite and stibiotantalite from Szklary; circles denote stibiocolumbite coexisting with CGM; diamonds denote stibiocolumbite coexisting with holtite; squares stand for a discrete grain of stibiotantalite and relict grains of stibiocolumbite–stibiotantalite in aggregates of PGM. (**b**) Variation of Bi/(Bi+Sb) in stibiocolumbite vs. Mn/(Mn+Fe) in the coexisting CGM.

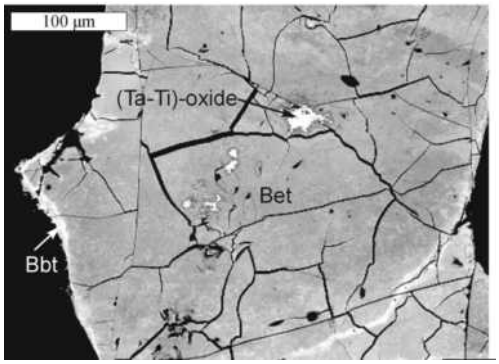

FIGURE 7. Inclusion of unnamed (As,Sb,U)-rich (Ta,Ti)-oxide in betafite mantled by Bi-dominant betafite; BSE image. Abbreviations: Bet = betafite, Bbt = Bi-dominant betafite.

native arsenic disseminated in microcline. Holtite is sometimes interspersed with bismutomicrolite (Fig. 8d). Stibiocolumbite occurs locally in interstices among holtite crystals or forms larger aggregates enclosing holtite (Figs. 8b–8c).

The holtite crystals show distinct zoning with a core comprising holtite proper (Ta-dominant) and a few-micrometers-wide rim composed of a Nb-dominant variety. In some samples, the core is heterogeneous and contains streaks of dark-gray color in BSE, at most 5 µm wide, representing a Ti-enriched or even Ti-dominant variety (Table 7). Irregular zones of Ti-bearing holtite are occasionally located at the margin between the Ta-dominant core and the Nb-dominant rim (Fig. 8). The Ta-dominant holtite has a Ta/(Nb+Ta) value ranging between 0.45 and 0.90, the Ti-dominant variety between 0.07 and 0.85, and, in the Nb-dominant rim, values are between 0.03 and 0.49.

TABLE 6. Representative compositions of an unnamed (As,Sb,U)-rich (Ta,Ti)-oxide from the Szklary pegmatite

	Sz25/1	Sz25/2	Sz26
		wt%	
WO_3	0.40	0.00	0.00
Nb_2O_5	7.01	6.97	6.85
Ta_2O_5	17.84	18.11	21.22
TiO_2	8.86	8.19	7.13
ZrO_2	0.00	0.00	0.00
SnO_2	0.00	0.00	0.00
ThO_2	1.16	1.09	0.88
UO_2	20.04	20.30	20.34
As_2O_3	12.69	11.18	11.93
Sb_2O_3	16.83	18.96	17.36
Bi_2O_3	0.34	0.47	0.62
FeO	2.83	2.50	2.19
MnO	9.83	9.76	9.87
MgO	0.00	0.00	0.00
CaO	0.34	0.31	0.32
PbO	0.94	1.08	0.82
Na_2O	0.05	0.09	0.06
K_2O	0.05	0.03	0.04
Total	99.19	99.05	99.66
		Atomic contents*	
W^{6+}	0.027	0.000	0.000
Nb^{5+}	0.828	0.837	0.826
Ta^{5+}	1.266	1.309	1.538
Ti^{4+}	1.739	1.638	1.430
Zr^{4+}	0.000	0.000	0.000
Sn^{4+}	0.000	0.000	0.000
U^{4+}	1.164	1.201	1.206
Th^{4+}	0.069	0.066	0.053
As^{3+}	2.011	1.805	1.930
Sb^{3+}	1.813	2.080	1.909
Bi^{3+}	0.023	0.033	0.043
Fe^{2+}	0.617	0.557	0.488
Mn^{2+}	2.174	2.198	2.228
Mg^{2+}	0.000	0.000	0.000
Ca^{2+}	0.096	0.088	0.092
Pb^{2+}	0.066	0.077	0.059
Na^{+}	0.024	0.044	0.030
K^{+}	0.018	0.012	0.015
Σcations	11.932	11.945	11.848
O^{2-}	20	20	20
Mn/(Mn+Fe)	0.779	0.798	0.820
Ta/(Ta+Nb)	0.605	0.610	0.651

Note: 0.00 wt% = a content below the respective detection limit.
* Based on 20 O apfu.

Alteration products of the primary Nb-Ta minerals

Alteration products of the primary Nb-Ta minerals in the Szklary pegmatite include fersmite and various members of the pyrochlore group, such as pyrochlore, bismutopyrochlore sometimes grading to plumbopyrochlore, stibiomicrolite, bismutomicrolite, uranmicrolite, betafite, and a previously unknown Bi-dominant variety of betafite (Table 8). All of these minerals contain SiO_2 in varying to extremely high amounts.

Fersmite, $(Ca,Ce,Na)(Nb,Ta,Ti)_2(O,OH,F)_6$, replaces columbite-(Mn) or crystals of columbite-(Fe) overgrown by columbite-(Mn) (Figs. 2d and 2g). Calcium is the major component in the A site (Table 8). It is accompanied by small amounts of Mn, Fe, Ba, sometimes Bi, and traces of U, Sb, and REE.

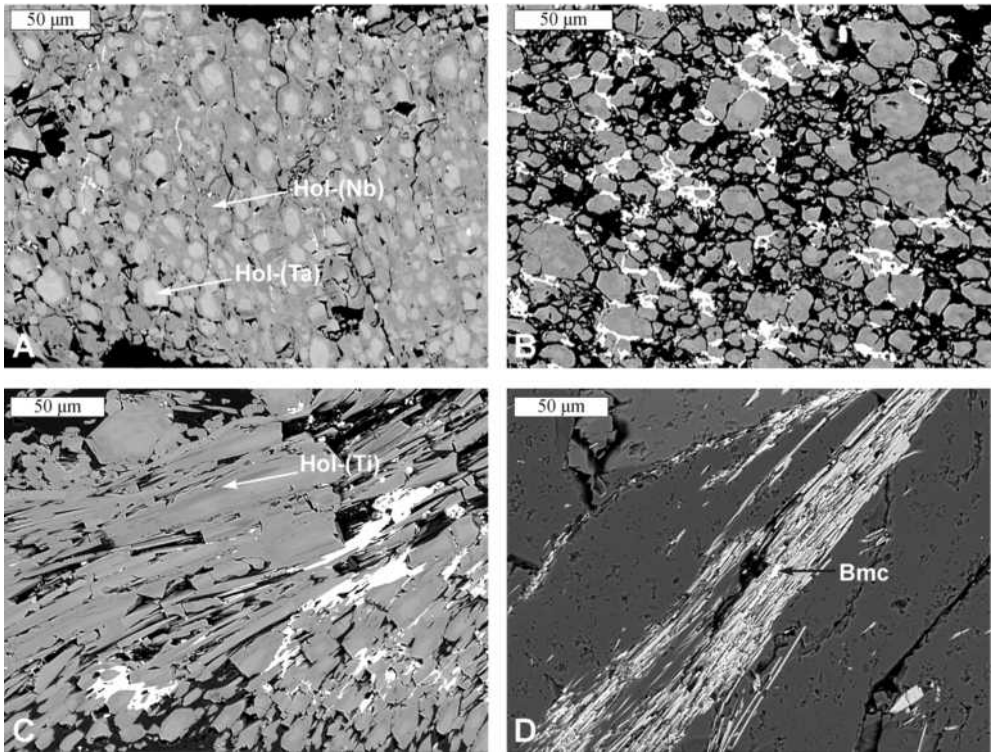

FIGURE 8. Typical textures exhibited by holtite from the Szklary pegmatite: (**a**) crosswise sections of holtite crystals showing a distinct Ta-dominant core and Nb-dominant rim; (**b**) stibiocolumbite (white) developed in interstices among holtite crystals; (**c**) longitudinal sections of zoned holtite crystals showing streaks of Ti-dominant holtite (dark gray) within the crystals, and interstitial stibiocolumbite (white); (**d**) aggregate of acicular holtite crystals with thin intercalations of bismutomicrolite. Abbreviations: Hol-(Ta) = Ta-dominant holtite, Hol-(Nb) = Nb-dominant holtite, Hol-(Ti) = Ti-dominant holtite, Bmc = bismutomicrolite.

The B site is occupied mainly by Nb, with the Ta/(Nb+Ta) ratio ranging from 0.08 to 0.20. Tungsten and Ti contents are relatively high, reaching 2.8 wt% WO_3 and 3.0 wt% TiO_2. The Si content ranges from below the detection limit to a few tenths of wt% SiO_2. Fersmite, coexisting with a crystal of altered zircon, is enriched in Zr (up to 0.6 wt% ZrO_2), but other fersmite crystals do not contain detectable zirconium.

The pyrochlore group is a diverse group of Nb-Ta-Ti oxides with the general formula $A_{2-m}B_2X_6Y_{1-n}{\cdot}pH_2O$, where A = Na, Ca, Mn^{2+}, Fe^{2+}, Mg, Sr, Sb, Cs, Ba, K, REE, Pb, Bi, U, and Th; B = Nb, Ta, Ti, W, Sn, Zr, Al, and Fe^{3+}; X = O and OH; and Y = F, OH, and O (Hogarth 1977). It is assumed that the B site is completely filled by cations and, therefore, formulae of these minerals are typically normalized to 2 B-site cations (Ercit et al. 1993). The A and Y sites commonly contain a significant proportion of vacancies (m = 0–1.7 and n = 0–1) stabilized by the incorporation of hydroxyls and H_2O molecules (p = 0–2). The EMPA data for Si-bearing pyrochlore-group minerals cannot be recalculated to a reliable structural formula because only a part of the Si detected by EMPA enters the B site, with the remaining part probably located in radiation-damaged parts of the structure (Bonazzi et al. 2006).

Pyrochlore has been found in the outermost zones of fersmite grains developed around grains of CGM (Fig. 2d). At Szklary, pyrochlore also occurs as the main product of alteration of columbite-(Mn) (Fig. 2g) or stibiocolumbite (Fig. 3b). Bismutopyrochlore locally overgrows crystals of CGM (Fig. 2f), forms veinlets penetrating earlier-crystallized CGM and fersmite (Fig. 2d), or small patches within crystals of CGM and pyrochlore (Figs. 2d and 2h). The A site is dominated by Ca (pyrochlore), Bi (bismutopyrochlore), and rarely Pb (plumbopyrochlore); other A-site components are subordinate. The Ta/(Ta+Nb) ratio is rather low, ranging from 0.12 to 0.14 in pyrochlore, and from 0.23 to 0.25 in Bi-rich plumbopyrochlore and bismutopyrochlore. The TiO_2 content varies from 3.5 wt% in pyrochlore coexisting with columbite-(Fe) and fersmite (Fig. 3d) to about 1.0 wt% in pyrochlore containing relics of columbite-(Mn) (Fig. 2h). The W content is typically about or below 1.0 wt% WO_3. Silicon is present in concentrations varying from about 1.0 wt% SiO_2 in pyrochlore, to 3.0–4.0 wt% SiO_2 in Bi-enriched pyrochlore, and to 5.0–6.0 wt% SiO_2 in bismutopyrochlore and Bi-rich plumbopyrochlore. The columbite-(Mn) replaced by pyrochlore (Fig. 2h) shows a very high Mn/(Mn+Fe) ratio close to 0.96 and a low Ta/(Ta+Nb) value close to 0.06.

Members of the microlite subgroup were identified among alteration products of stibiotantalite (Figs. 5d–5e). Bismutomicrolite has also been found as interspersions in holtite aggregates (Fig. 8d). The A site in these minerals is dominated by Bi (bismutomicrolite), Sb (stibiomicrolite), or U (uranmicrolite), but stibiomicrolite and bismutomicrolite do not coexist. The Ta/(Ta+Nb) ratio in the microlite (0.64–0.80) is comparable to that in the coexisting stibiotantalite (Table 5). Titanium content in bismutomicrolite is very low, clearly below 1.0 wt% TiO_2 and somewhat higher in stibiomicrolite (ca.1.0 wt%). However, in the

TABLE 7. Representative compositions of holtite from the Szklary pegmatite

Sz32	Core	Strips	Rim
		wt%	
P_2O_5	0.58	0.00	0.00
Nb_2O_5	0.68	3.58	5.30
Ta_2O_5	7.02	0.67	1.06
SiO_2	17.69	18.90	17.88
TiO_2	1.23	2.16	0.95
B_2O_3*	5.17	5.33	5.30
Al_2O_3	47.04	48.00	47.55
As_2O_3	3.24	2.14	2.14
Sb_2O_3	14.46	17.42	18.25
FeO	0.13	0.19	0.22
Total	97.24	98.40	98.63
		Atomic contents†	
$^{VI}Al^{3+}$	6.147	6.127	6.089
Nb^{5+}	0.034	0.176	0.263
Ta^{5+}	0.214	0.020	0.032
Ti^{4+}	0.104	0.177	0.079
Fe^{2+}	0.012	0.017	0.021
$\square_{cat.}$	0.489	0.483	0.549
B^{3+}	1.000	1.000	1.000
Si^{4+}	1.984	2.054	1.964
P^{5+}	0.055	0.000	0.000
$^{IV}Al^{3+}$	0.071	0.022	0.066
As^{3+}	0.221	0.142	0.143
Sb^{3+}	0.669	0.782	0.827
O^{2-}	17.110	17.076	17.030
$\square_{an.}$	0.890	0.924	0.970

Note: 0.00 wt% = a content below the respective detection limit; □ = vacancy.
* Calculated by stoichiometry.
† Based on $O = (18 - N_{Sb} - N_{As})$ apfu.

uranmicrolite associated with stibiomicrolite, the TiO_2 content reaches nearly 7.2 wt%, and is closer to that in the coexisting betafite (11.0 wt% TiO_2). Tungsten commonly is present in concentrations much lower than 1.0 wt% WO_3. SiO_2 content is rather low, ranging from 1.0 to 4.0 wt%, but in the Ti-bearing bismutomicrolite coexisting with uranmicrolite (Fig. 5f), SiO_2 reaches 11.3 wt%.

Betafite and a Bi-dominant variety of betafite are the most common PGM in the Szklary pegmatite. Betafite overgrows relict stibiotantalite with stibiomicrolite and uranmicrolite (Fig. 5e), or relict grains of the (As,Sb,U)-rich (Ta,Ti)-oxide (Fig. 7). In betafite, the Ta/(Ta+Nb) ratio ranges from 0.65 to 0.77, and the Ta/(Ta+Ti) ratio from 0.43 to 0.49, showing continuity with Ti-bearing uranmicrolite (0.77–0.80, 0.55–0.60, respectively). The betafite is enriched in Sb (6.0–7.0 wt% Sb_2O_3) and Ba (to 3.5 wt%), but is rather poor in Bi (~1.0 wt% Bi_2O_3). The SiO_2 is low in most samples, ranging between 2.0 and 3.0 wt%, but in the stibiotantalite–stibiomicrolite–uranmicrolite to betafite aggregate, the content of SiO_2 in the outermost enriched in Bi parts dramatically increases to above 18.0 wt%, a content slightly higher than the highest SiO_2 level in a pyrochlore-group mineral known in nature (Chakhmouradian and Mitchell 2002). A transitional member between Sb-bearing betafite and Bi-dominant variety of this mineral forms a thin rim around betafite enclosing the (As,Sb,U)-rich (Ta,Ti)-oxide (Fig. 7). The Bi-dominant variety of betafite as an overgrowth on stibiocolumbite contains up to 36.5 wt% B_2O_3 in the rim, and up to 19.0 wt% Bi_2O_3 in internal patches (Fig. 5g). The Ta/(Ta+Nb) ratio of this mineral, ranging from 0.41 to 0.46, is higher than the value in the coexisting stibiocolumbite. Also notable are its high SiO_2 and ZrO_2 contents reaching 13.5 and 2.1 wt%, respectively, in the rim and 18.0 and 3.4 wt% in the patches.

DISCUSSION

The Szklary dike crystallized from an anatectic, highly evolved, B- and Cl-enriched peraluminous melt carrying REE

TABLE 8. Representative compositions of fersmite and pyrochlore-group minerals from the Szklary pegmatite

	SzA*		Sz11		Sz18			Sz2b		Sz5-b			Sz18			Sz13		Sz27		Sz26	
	Fsm	Fsm-a	Fsm-b	Pyr	Ppy	Bpy	Pyr	Pyr	Pbp	Bmc	Bmc	Stm	Umc	Bet	Bbt	Umc	Bmc	Bbt†	Bbt‡	Bet	Bbt
												wt%									
WO_3	1.53	2.83	2.43	1.66	0.54	0.22	1.06	1.19	0.34	0.00	0.00	0.54	0.13	0.16	0.39	1.00	1.30	0.44	0.38	0.62	0.38
Nb_2O_5	61.84	63.83	57.14	56.12	31.11	20.79	53.80	49.44	39.59	12.70	7.09	7.96	4.45	4.15	5.30	5.18	6.32	9.57	10.30	7.89	7.92
Ta_2O_5	14.86	11.98	20.75	13.40	15.31	11.89	9.63	12.76	10.26	37.19	42.51	44.52	29.62	22.52	33.05	29.45	38.75	11.01	14.46	24.32	18.47
SiO_2	0.79	0.35	0.24	1.19	6.17	5.47	3.05	3.06	3.95	4.24	3.54	1.17	1.71	2.14	18.13	3.06	10.70	13.57	18.00	3.33	2.74
TiO_2	1.34	3.01	2.74	3.52	2.41	1.00	1.06	1.08	0.83	0.30	0.19	0.96	7.16	10.98	12.43	8.80	11.34	13.70	15.99	9.14	8.65
ZrO_2	0.00	0.26	0.00	0.26	0.20	0.00	0.00	0.00	0.00	0.00	0.00	0.00	0.00	0.00	0.24	0.00	0.34	2.14	3.40	0.00	0.00
SnO_2	0.00	0.00	0.00	0.00	0.00	0.00	0.00	0.00	0.00	0.00	0.00	0.00	0.00	0.00	0.00	0.00	0.15	0.00	0.00	0.00	0.00
ThO_2	0.00	0.00	0.00	0.00	0.00	0.00	0.00	0.00	0.00	0.00	0.00	0.00	0.30	0.17	0.85	0.50	0.65	0.00	0.00	1.21	0.95
UO_2	0.26	0.00	0.00	0.25	2.59	1.82	0.65	0.58	1.11	0.87	1.22	4.19	27.29	27.54	1.80	24.77	2.10	2.44	1.93	24.79	17.85
Al_2O_3	0.06	0.00	0.00	0.00	0.69	0.68	0.00	0.12	0.35	0.60	0.45	0.00	0.00	0.04	1.12	0.00	0.56	0.69	0.99	0.00	0.18
As_2O_3	0.46	0.00	0.00	0.00	0.00	0.00	0.00	0.00	0.00	0.00	0.08	1.57	2.09	0.93	0.00	2.07	0.00	0.00	0.00	3.25	0.32
Sb_2O_3	0.43	0.00	0.00	0.00	0.13	1.97	0.44	0.47	1.29	4.53	4.93	15.95	8.33	7.19	0.31	7.46	4.03	0.44	0.26	6.11	4.39
Bi_2O_3	1.28	0.00	0.00	1.60	10.12	31.99	11.55	11.01	16.84	26.87	21.84	2.13	1.70	1.22	5.46	0.20	12.41	36.51	18.97	0.99	16.64
Sc_2O_3	0.00	0.00	0.00	0.00	0.00	0.00	0.00	0.00	0.00	0.15	0.19	0.00	0.00	0.00	0.05	0.00	0.04	0.03	0.00	0.00	0.00
MgO	0.16	0.04	0.03	0.18	0.75	0.58	0.41	0.39	0.64	0.44	0.51	0.28	0.10	0.18	0.85	0.16	0.40	0.48	1.00	0.00	0.33
CaO	13.98	15.59	14.89	12.76	2.49	2.24	8.46	8.03	3.66	2.57	1.95	3.07	2.38	3.20	2.01	3.01	1.05	1.16	1.55	3.94	1.02
MnO	0.71	0.34	0.44	0.28	0.33	1.39	1.44	1.63	1.95	0.89	0.61	1.20	0.97	0.18	0.00	1.70	0.83	0.19	0.22	1.90	0.42
FeO	0.37	0.39	0.62	0.59	0.51	3.61	1.01	0.95	1.14	0.76	0.83	1.10	1.06	0.91	1.19	0.76	2.27	0.60	0.43	1.51	1.63
BaO	0.79	0.28	0.00	1.39	1.36	0.37	0.89	0.87	0.87	1.49	1.15	3.51	1.48	3.22	2.83	2.48	1.03	0.48	1.09	0.62	1.42
PbO	0.00	0.00	0.00	0.96	18.28	7.12	2.61	5.03	13.16	0.43	8.29	0.65	0.97	0.81	2.96	0.17	2.68	1.28	1.35	0.74	2.83
Na_2O	0.05	0.04	0.00	0.04	0.08	0.00	0.03	0.06	0.05	0.07	0.00	0.00	0.00	0.00	0.00	0.00	0.00	0.00	0.00	0.00	0.00
K_2O	0.00	0.00	0.00	0.00	0.00	0.00	0.00	0.00	0.00	0.00	0.00	0.03	0.26	0.14	0.00	0.19	0.00	0.00	0.04	0.11	0.07
Total	99.35	99.14	99.28	94.68	93.06	91.14	96.09	96.68	96.04	94.09	95.40	88.80	89.94	85.68	88.97	90.85	96.96	94.71	90.37	90.46	86.21
Ta/(Ta+Nb)	0.126	0.101	0.179	0.126	0.228	0.256	0.097	0.134	0.135	0.638	0.783	0.771	0.800	0.766	0.790	0.774	0.787	0.409	0.458	0.649	0.584
Ta/(Ta+Ti)	0.801	0.590	0.733	0.579	0.697	0.811	0.767	0.810	0.816	0.978	0.988	0.944	0.599	0.426	0.490	0.548	0.552	0.225	0.246	0.490	0.435

Note: 0.00 wt% = a content below the detection limit. Abbreviations: Fsm = fersmite, Pyr = pyrochlore, Ppy = plumbopyrochlore, Bpy = bismutopyrochlore, Pbp = Pb-rich bismutopyrochlore, Bmc= bismutomicrolite, Stm = stibiomicrolite, Umc = uranmicrolite, Bet = betafite, Bbt = Bi-dominant betafite.
* The analyses show 0.00, 0.18, 0.00, and 0.33 wt% Y_2O_3, and 0.45, 0.00, 0.00, and 0.15 wt% Ce_2O_3, respectively.
† Rim.
‡ Internal patchy zones.

and high-field-strength metals in the form of phosphate, fluoride, and chloride complexes. On cooling, cheralite, xenotime-(Y), Hf-bearing zircon, chrysoberyl, and primary Nb and Ta minerals crystallized from the melt at an early stage. Figure 9 presents the generalized conditions of crystallization of the primary Nb and Ta minerals in the Szklary pegmatite in terms of Mn-Fe and Ta-Nb fractionation.

The compositional trends exhibited by CGM share a number of important features. Columbite-(Mn), whose compositions plot at the beginning of trends I and II, shows a decrease in Mn/(Mn+Fe) ratio from 0.85 to 0.78, and from 0.78–0.79 to 0.70–0.72, respectively. Trend III, beginning with the crystallization of columbite-(Fe), also involves a slight decrease in Mn/(Mn+Fe) ratio (from 0.44 to 0.42). In all three cases, the decrease in Mn/(Mn+Fe) is accompanied, not only by an increase in the proportion of Fe, but also by progressive enrichment in Mg (Fig. 4a). Columbite-(Mg) and tantalite-(Mg), the Mg-dominant members of the columbite group, were found in pegmatites hosted by Mg-rich rocks (dolomitic marble and serpentinite, respectively; Mathias et al. 1963; Pekov et al. 2003). The enrichment in Fe and Mg in columbite-(Fe), which is the earliest-crystallized Nb and Ta oxide, and in the core of columbite-(Mn) crystals, is a result of contamination of the pegmatite-forming melt by material from the ultramafic and mafic wall-rocks. Additional evidence of such contamination includes the crystallization of biotite, abundant in the border zone, through a reaction of the pegmatite melt with the wall-rock serpentinite and amphibolite, and enrichment of black tourmaline in Mg (Pieczka and Kraczka 1996; Pieczka 2007a). Tourmaline crystals from the border zone contain up to 6.46 wt% MgO (1.58 Mg apfu) compared up to 3.89 wt% MgO (0.97 Mg apfu) in those from the inner zone. The crystallization of columbite-(Fe) and, to some extent, columbite-(Mn) took place under crystal/melt disequilibrium, which resulted in a patchy texture in the core, in contrast to other crystals of columbite-(Mn) showing a regular zoning, formed under crystal/melt equilibrium.

Subsequent crystallization of CGM in the Szklary pegmatite was accompanied by a sharp increase in Ta content at constant or slightly increasing levels of Mn, which resulted in the formation of the Ta-rich rim on, or fracture-filling veinlets in, earlier-formed crystals (Fig. 2). The accumulation of Ta in the melt and the late crystallization of tantalite-(Mn) are a result of the higher solubility of $MnTa_2O_6$ relative to of $MnNb_2O_6$ in silicate melts (Keppler 1993; Linnen and Keppler 1997; Linnen 1998). The available textural evidence (Fig. 2) and drastic changes in composition across the core-rim boundary indicate that the precipitation of Ta-rich columbite-(Mn) evolving to tantalite-(Mn) occurred after a crystallization gap, rather than immediately after the formation of the early columbite.

The synchronous crystallization of Ta-bearing columbite-(Mn) or tantalite-(Mn), Ta-bearing stibiocolumbite, evolving to stibiotantalite, and Ta-dominant holtite under the conditions close to the peak Ta-enrichment in the melt is consistent with the observations of Černý et al. (2004) for Nb, Ta, Sn, and Sb oxide minerals from the Varuträsk pegmatite, Sweden. In the Szklary pegmatite, the crystallization led to a decrease in Ta/(Ta+Nb) ratio and, as a result, renewed crystallization of Ta-poor columbite-(Mn) at slightly higher levels of Mn/(Mn+Fe). This newly formed columbite-(Mn) occurs as overgrowths on the Ta-bearing rim of CGM crystals. The decrease in Ta availability also resulted in alteration of the early stibiocolumbite to stibiocolumbite with lower Ta/(Ta+Nb) values, whereas holtite, also crystallizing at this stage, is zoned and shows a distinct decrease in Ta/(Ta+Nb) from ca. 0.90 in the core to 0.03 in the rim. The enrichment in Ti in the Ta-dominant core of the holtite crystals and the predominance of Ti over Ta and Nb in the Ti-dominant streaks indicate a link between holtite and local crystallization environments corresponding to trend II in the CGM.

Zoning in CGM is commonly considered as an indication of their crystallization and fractionation from melt. The compositional trends observed in the CGM from the Szklary pegmatite, showing highly variable (increasing or decreasing) Mn/(Mn+Fe) and Ta/(Ta+Nb) ratios, are also controlled by variations in the composition of the parental melt. However, what magmatic processes can be responsible for such different compositional trends? A decrease in Mn and/or Ta contents in Nb-Ta minerals precipitating from an evolving melt is not commonly observed, but has been reported from a number of pegmatites. Fersman (1940), studying the bulk composition of CGM, first noted a decrease in Ta content in crystals from more evolved pegmatite parageneses relative to crystals from the earlier-formed parageneses. Kornetova (1961) described a similar trend. Subsequently, the anomalous pattern of decreasing Ta and/or Mn content was reported in columbite-(Mn) replaced by tantalite-(Fe) in the

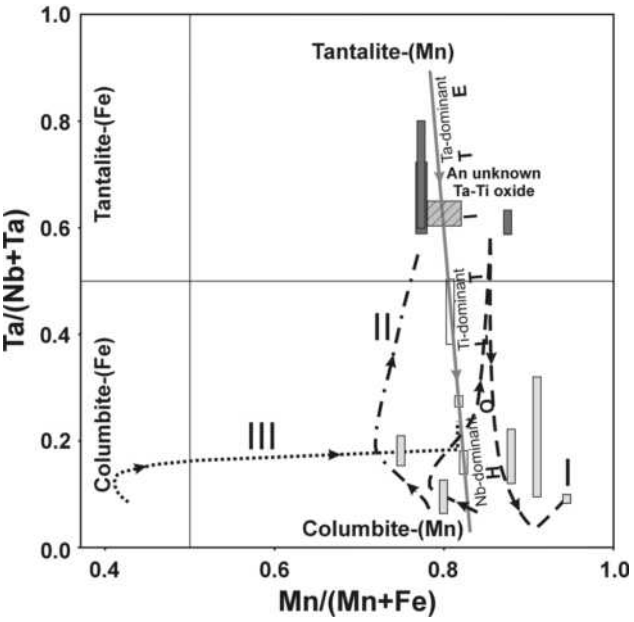

FIGURE 9. Summary paragenetic-chemical diagram showing relationships among the primary Nb-Ta minerals in the Szklary pegmatite in terms of Mn-Fe and Ta-Nb fractionation. The three compositional trends exhibited by the CGM are indicated by the dashed line (trend I), dotted-dashed line (trend II), and dotted line (trend III), fractionation trend in holtite is denoted by the dark gray solid line; other symbols show the compositional fields of stibiocolumbite coexisting with the CGM (light gray rectangles), stibiocolumbite (dark gray rectangles), stibiotantalite coexisting with holtite (white rectangles), (As,Sb,U)-rich (Ta,Ti)-oxide (gray lined rectangle).

Rubicon pegmatite, Namibia (Baldwin 1989), in columbite-(Mn) replaced by columbite-(Fe) at Rožná, Czech Republic (Novák and Černý 2001), and in CGM from a beryl-columbite pegmatite at Scheibengraben, Czech Republic (Novák et al. 2003). In other Nb- and Ta-bearing minerals, an inverse path of Mn-Fe and/or Ta-Nb fractionation was described for Ta-rich ixiolite and columbite-(Mn) evolving to tantalite-(Mn) in the Lower Tanco pegmatite, Canada (Ferreira 1984), alteration products of simpsonite (Ercit 1986), holtite replaced by ferrotapiolite (Voloshin and Pakhomovskyi 1988), products of stibiotantalite replacement from Moldanubicum, Czech Republic (Novák and Černý 1998), and in stibiotantalite replaced by ferrotapiolite in the Laštovičky pegmatite, Czech Republic (Novák et al. 2004). The atypical decrease in Mn and/or Ta in Nb-Ta minerals during crystallization has been termed "reversed" fractionation (e.g., Černý et al. 1985).

Considering the small thickness of the Szklary dike, and especially of its inner zone containing the described Nb-Ta minerals, it is almost certain that the anomalies in Mn-Fe and Ta-Nb fractionation can be readily explained by contamination of the parental melt by material from the ultramafic and mafic wall-rocks, competition of the primary oxide minerals for these elements, local variations in melt composition, and late-stage alteration processes. Although the CGM in the Szklary pegmatite originate from the feldspar-quartz graphic intergrowths of the inner zone and their compositional variation can be a complex result of the above-mentioned processes, a crystallization "gap" between columbite-(Fe) and columbite-(Mn) indicates that co-crystallizing biotite and schorl could strongly deplete the melt of Fe, Mg, and Ti, interrupting the precipitation of CGM. Thus, the compositional variation of the CGM, apart from being the result of melt fractionation, records competitive partitioning of elements between these minerals, biotite, and tourmaline. Crystallization of the latter minerals effectively drove the compositional evolution of CGM toward enrichment in Mn and Ta, and depletion in Mg and Ti.

It is worth noting that Ta fractionation reached a similar level in the CGM following trends I and II [Ta/(Ta+Nb) ~ 0.60]. Then, the crystallization of tantalite-(Mn) ceased despite the presence of Ta in the melt, or the Ta content decreased drastically producing successive zones of columbite-(Mn) with a slightly higher value of Mn/(Mn+Fe). The main reason for the gap in the crystallization of tantalite-(Mn) might be enrichment in the melt of Sb, Bi, and As, which compete with Mn and Fe for Ta and, thus, control the crystallization of CGM vs. SCGM.

Members of the stibiocolumbite-stibiotantalite series are accessory components of many pegmatites hosting Nb-Ta minerals. In the Szklary pegmatite, the Ta/(Ta+Nb) ratio in stibiocolumbite is always slightly higher than that in the coexisting columbite-(Mn). However, in stibiotantalite, that ratio reaches 0.80, which is much higher than in the Ta-richest tantalite-(Mn). It may be argued that a high Sb activity in the system facilitated the crystallization of stibiotantalite instead of tantalite-(Mn). In addition, the compositional field of $(Mn_3U)As_2Sb_2Ta_2Ti_2O_{20}$ plotted in terms of Ta/(Ta+Nb) and Mn/(Mn+Fe) values is a continuation of trend II in columbite-(Mn) evolving to tantalite-(Mn), and indicates an appreciable increase in Fe, Ti, and U contents. The association of Mn, U, As, Sb, Ti, and Ta is unique, which explains why neither all nor even any four of these six elements have been previously reported to occur in significant concentrations in the same mineral. This brings up the question why tantalite-(Mn) or stibiotantalite did not crystallize in place of $(Mn_3U)As_2Sb_2Ta_2Ti_2O_{20}$ under these conditions. One possible explanation is that the latter oxide phase is more stable than tantalite-(Mn) or stibiotantalite in the presence of abundant U^{4+}, Ti^{4+}, and As^{3+}.

The complex chemistry of the melt that gave rise to the Szklary pegmatite (i.e., its enrichment in Ta, Nb, Sb, and As, in addition to such typical lithophile components as Si, Al, Ti, and B, as well as the dearth of sulfur) may be the main reason for crystallization of holtite at this locality. The Szklary dike is one of three occurrences worldwide where this mineral coexists with (Nb,Ta)-oxides (Pieczka and Marszałek 1996). The other two localities are an alluvial tin deposit near Greenbushes in south-western Western Australia (Pryce 1971), and a pegmatite at Mount Vasin-Myl'k, Voron'i Tundry, Kola Peninsula, Russia (Voloshin et al. 1977). At both of these occurrences, holtite is associated with stibiotantalite, whereas at the Szklary it is associated with stibiocolumbite. Furthermore, the Australian holtite is a secondary phase formed by alteration of stibiotantalite (Pryce 1971). In the Szklary pegmatite, the core of holtite crystals is invariably richer in Ta than the rim, recording a decrease in Ta activity in the melt during crystallization of this mineral, similar to the late columbite-(Mn) or stibiocolumbite. Stibiocolumbite occurs locally in interstices between holtite crystals or forms aggregates enclosing holtite. This stibiocolumbite commonly shows relatively little Ta-Nb fractionation, suggesting that Nb-dominant holtite and late stibiocolumbite crystallized almost simultaneously over a very narrow range of Mn/(Mn+Fe) values. The holtite-stibiocolumbite textural relationships and zoning in the holtite crystals unequivocally indicate that holtite is a primary Nb-Ta mineral crystallizing along with stibiocolumbite under the conditions corresponding to the descending branch of the Ta-enrichment peak (Fig. 9). Additionally, Szklary is the only known locality where Ta-, Nb-, and Ti-dominant varieties of holtite coexist.

The early crystallization of volatile-free minerals resulted in a gradual build-up of volatiles in the melt followed by exsolution of an aqueous fluid that carried various elements (Ca, Mn, Fe, Ba, Pb, Bi,...) mainly as fluoride and chloride complexes. The fluid induced subsolidus metasomatic processes in the pegmatite, initiated alteration of the primary Nb-Ta oxides into fersmite and members of the pyrochlore group. The crystal of columbite-(Fe) evolving to columbite-(Mn) (Fig. 2d), with Ta/(Ta+Nb) ratio ranging from 0.09 to 0.24, was altered from the margin into fersmite [Ta/(Ta+Nb) = 0.10–0.18] and pyrochlore, (ca. 0.13). Bismuth-rich plumbopyrochlore, forming veinlets and patches in both the CGM and pyrochlore, has Ta/(Ta+Nb) ratio close to 0.23. Columbite-(Mn), whose Ta/(Ta+Nb) ratio increases from 0.05 in the core to 0.10 in the rim (Fig. 2g), was altered into fersmite (0.12–0.13), whereas columbite-(Mn) (Fig. 2h), with Ta/(Ta+Nb) close to 0.06, was replaced by pyrochlore (0.10–0.13). Similarly, the (As,Sb,U)-rich (Ta,Ti)-oxide with Ta/(Ta+Nb) ≈ 0.60–0.65 was altered to a Ta-bearing betafite (~0.65) and rimmed by Bi-bearing betafite (~0.58). Stibiocolumbite (Fig. 3g) with Ta/(Ta+Nb) ~ 0.34 was altered into Bi-dominant betafite (0.41–0.46). Stibiotantalite (Figs. 5d–5f) with Ta/(Ta+Nb) =

0.59 to 0.74 was replaced by bismutomicrolite (0.64–0.78), or uranmicrolite and bismutomicrolite (0.77–0.79), or stibiomicrolite (0.77), uranmicrolite (0.80), and subsequently betafite (0.77) and Bi-bearing betafite (0.79). In all of these secondary PGM minerals, the extent of Ta-Nb fractionation is comparable to, or only slightly greater than, the primary Nb-Ta oxides, indicating further evolution of a residual melt coexisting with the fluid.

The PGM from Szklary typically show a patchy texture in BSE images, arising from variations in Si content. There is little information on Si-rich PGM available in the literature, even though they were first described more than 100 years ago (Flink 1898, 1901) in nepheline syenite at Narssârssuk (Greenland). This "silicified" pyrochlore contains up to 11.5 wt% SiO_2 (Bonazzi et al. 2006). Johan and Johan (1994) described U-enriched PGM containing 7.4 to 10.1 wt% SiO_2 from the Zinnwald granite, Czech Republic, and Uher et al. (1998) reported microlite with 8.6–9.5 wt% SiO_2 in granitic pegmatites at Prašivá, Slovakia. Pyrochlore, with exceptionally high contents of SiO_2, reaching 16.8 wt%, was reported from metasomatic rocks of the Lovozero alkaline complex, Russia (Chakhmouradian and Mitchell 2002). Ercit et al. (2003) described bismutopyrochlore with 10.5 wt% SiO_2 from pegmatites of the O'Grady batholith, Northwest Territories, Canada, and Černý et al. (2004) measured up to 8.2 wt% SiO_2 in metasomatic members of the pyrochlore and microlite subgroup from the Varuträsk pegmatite. All of the Si-rich PGM reported in the literature give a large proportion of vacancies in the A site and low analytical totals. On the basis of a negative correlation between Si and Σ(Nb,Ta,W,Ti,Sn,Zr), Johan and Johan (1994), Uher et al. (1998), and Chakhmouradian and Mitchell (2002) suggested that Si is incorporated in the B site of the pyrochlore structure. In contrast, Möller et al. (2001) suggested that Si could enter the A site, whereas several other authors have proposed that high Si content could reflect the presence of silicate impurities (e.g., Hogarth 1977, 1989; Hogarth et al. 2000), or amorphous silica (Voloshin et al. 1989). The only example of Si-rich pyrochlore with a refined crystal structure is the cotype material from Narssârssuk (Bonazzi et al. 2006). A detailed structural study of this material showed that only about 30–50% of the Si detected by EMPA is incorporated in the B site, whereas the remaining 50–70% is localized in radiation-damaged portions of the structure.

The Si contents of the PGM formed by alteration of the earlier-crystallized Nb-Ta oxides in the Szklary pegmatite, is highly variable. Pyrochlore, uranmicrolite, and stibiomicrolite contain trace amounts of Si (1–2 wt% SiO_2), but many of the remaining members of the pyrochlore, microlite, and especially betafite subgroup contain high to very high levels of SiO_2. The highest SiO_2 contents, exceeding 20.0 wt%, were found in Bi- and Ca-dominant "betafite" with a large proportion of vacancies in the A site. These compositions are close to the empirical formula $^{A}(Ca_{0.2}Bi_{0.2}\square_{1.6})^{B}[SiTi_{0.5}(Ta,Nb)_{0.5}]^{X}(O_{3.5}OH_{2.5})^{Y}\square_{1.0}$, which can be interpreted either as a "silicified" member of the pyrochlore group or a hypothetical Bi- and Ti-enriched komarovite-like phase, i.e. $(Ca_{0.4}Bi_{0.4}\square_{0.2})(Ta,Nb)TiSi_2O_7O_2OH{\cdot}2H_2O$. The latter interpretation is in accord with the suggestion of Chakhmouradian and Mitchell (2002) that submicroscopic intergrowths of pyrochlore with komarovite could also explain the incorporation of Si in pyrochlore. Komarovite has a layered structure that consists of pyrochlore slabs connected by four-membered tetrahedral silicate rings (Krivokoneva et al. 1979; Balić-Žunić et al. 2002; Ferraris et al. 2004). Such intergrowths may be responsible for the presence of high levels of Si in PGM without having to invoke an atypical sixfold coordination environment for Si. However, the problem of the structural role of Si in PGM remains open and requires further submicrometer-scale structural study of these minerals.

A careful paragenetic analysis of the primary Nb-Ta minerals and products of their hydrothermal alteration in the Szklary pegmatite enabled to construct the following generalized crystallization sequences:

- columbite-(Fe) → columbite-(Mn) → tantalite-(Mn) [→ columbite-(Mn)],
- columbite-(Mn) → stibiocolumbite → stibiotantalite or (As,Sb,U)-rich (Ta,Ti)-oxide → Ta-dominant holtite → Nb-dominant holtite + stibiocolumbite,
- columbite-(Mn) → fersmite → pyrochlore → bismutopyrochlore → plumbopyrochlore,
- stibiocolumbite or stibiotantalite or (As,Sb,U)-rich (Ta,Ti)-oxide → stibiomicrolite → uranmicrolite to betafite → bismutomicrolite to Bi-dominant betafite.

ACKNOWLEDGMENTS

This work was financially supported by AGH, University of Science and Technology (grant no. 11.11.140.158). I thank S. Simmons, P. Uher, A. Chakhmouradian, and L.A. Groat for constructive comments that greatly improved the manuscript, and R. Macdonald and J.A. Thomson (Editor) for assistance in correcting the final version of the paper.

REFERENCES CITED

Baldwin, J.R. (1989) Replacement phenomena in tantalum minerals from rare-metal pegmatites in South Africa and Namibia. Mineralogical Magazine, 53, 571–581.

Balić-Žunić, T., Petersen, O.V., Bernhardt, H.J., and Micheelsen, H.I. (2002) The crystal structure and mineralogical description of a Na-dominant komarovite from the Ilímaussaq alkaline complex, South Greenland. Neues Jahrbuch für Mineralogie, Monatshefte, 11, 497–514.

Bonazzi, P., Bindi, L., Zoppi, M., Capitani, G.C., and Olmi, F. (2006) Single-crystal diffraction and transmission electron microscopy studies of "silicified" pyrochlore from Narassârssuk, Julianehaab district, Greenland. American Mineralogist, 91, 794–801.

Černý, P. and Ercit, T.S. (2005) The classification of granitic pegmatites revisited. Canadian Mineralogist, 43, 2005–2026.

Černý, P., Meintzer, R.E., and Anderson, A.J. (1985) Extreme fractionation in rare-element granitic pegmatites: Selected examples of data and mechanisms. Canadian Mineralogist, 23, 381–421.

Černý, P., Chapman, R., Ferreira, K., and Smeds, S.A. (2004) Geochemistry of oxide minerals of Nb, Ta, Sn, and Sb in the Varuträsk granitic pegmatite, Sweden: The case of "anomalous" columbite-tantalite trend. American Mineralogist, 89, 505–518.

Chakhmouradian, A.R. and Mitchell, R.H. (2002) New data on pyrochlore- and perovskite-group minerals from the Lovozero alkaline complex, Russia. European Journal of Mineralogy, 14, 821–836.

Ercit, T.S. (1986) The simpsonite paragenesis. The crystal chemistry and geochemistry of extreme Ta fractionation. Unpublished Ph.D. thesis, University of Manitoba.

Ercit, T.S., Černý, P., and Hawthorne, F.C. (1993) Cesstibtantite—a geological introduction in the inverse pyrochlores. Mineralogy and Petrology, 48, 235–255.

Ercit, T.S., Groat, L.A., and Gault, R.A. (2003) Granitic pegmatites of the O'Grady batholith, N.W.T., Canada: A case study of the evolution on the elbaite subtype of rare-element granitic pegmatite. Canadian Mineralogist, 41, 117–137.

Ferraris, G., Makovicky, E., and Merlino, S. (2004) Crystallography of modular materials. IUCr Monographs on Crystallography 15, Oxford University Press, New York.

Ferreira, K.J. (1984) The mineralogy and geochemistry of the Lower Tanco pegmatite, Bernic Lake, Manitoba, Canada. Unpublished M.Sc. thesis, University of Manitoba.

Fersman, A.E. (1940) Pegmatites. Reprinted in 1960 as Selected Works VI, Academy of Science, U.S.S.R., Moscow (in Russian).

Flink, G. (1898) Berättelse om en mineralogisk resa i Syd-Grönland sommaren

1897. Meddelelser om Grønland, 14, 221–261.
——— (1901) On the minerals from Narsarsuk on the Firth of Tunugdliarfik in southern Greenland. Meddelelser om Grønland, 24, 7–180.
Hogarth, D.D. (1977) Classification and nomenclature of the pyrochlore group. American Mineralogist, 62, 403–410.
——— (1989) Pyrochlore, apatite and amphibole: distinctive minerals in carbonatite. In K. Bell, Ed., Carbonatites: genesis and evolution, p. 105–148. Unwin Hyman, London.
Hogarth, D.D., Williams, C.T., and Jones, P. (2000) Primary zoning in pyrochlore group minerals from carbonatites. Mineralogical Magazine, 64, 683–697.
Johan, V. and Johan, Z. (1994) Accessory minerals of the Cínovec (Zinnwald) granite cupola, Czech Republic. 1. Nb, Ta- and Ti-bearing oxides. Mineralogy and Petrology, 51, 323–343.
Keppler, H. (1993) Influence of fluorine on the enrichment of high field strength trace element in granitic rocks. Contributions to Mineralogy and Petrology, 109, 139–150.
Kornetova, V.A. (1961) Some observations on the columbite-tantalite mineral group. Trudy Mineralogicheskogo Muzeya AN SSSR, 12, 65–69 (in Russian).
Krivokoneva, G.K., Portnov, A.M., Semenov, E.I., and Dubakina, L.S. (1979) Komarovite—a silicified pyrochlore. Doklady AN SSSR, Earth Science Sections, 248, 127–130.
Linnen, R.L. (1998) The solubility of Nb-Ta-Zr-Hf-W in granitic melts with Li and Li + F: Constraints for mineralization in rare metal granites and pegmatites. Economic Geology, 93, 1013–1025.
Linnen, R.L. and Keppler, H. (1997) Columbite solubility in granitic melts: consequences for the enrichment and fractionation of Nb and Ta in the Earth's crust. Contributions to Mineralogy and Petrology, 128, 213–227.
Majerowicz, A. and Pin, C. (1986) Preliminary trace element evidence for an oceanic depleted mantle origin of the Ślęża ophiolitic complex SW Poland. Mineralogia Polonica, 17, 12–22.
Mathias, V.V., Rossovskii, L.N., Shostatskii, A.N., and Kumskova, N.M. (1963) Magnocolumbite, a new mineral. Doklady AN SSSR, 148, 420–423 (in Russian).
Michalik, R. (2000) Gold in the serpentinite weathering cover of the Szklary massif, Fore-Sudetic Block, SW Poland. Geologia Sudetica, 33, 143–150.
Möller, T., Clearfield, A., and Harjula, R. (2001) The effect of cell dimensions of hydrous mixed metal oxides with a pyrochlore structure on the ion-exchange properties. Chemical Materials, 13, 4767–4772.
Niśkiewicz, J. (1967) Geological structure of the Szklary Massif (Lower Silesia). Journal of Polish Geological Society, 37, 387–414 (in Polish).
Novák, M. and Černý, P. (1998) Niobium-tantalum oxide minerals from complex granitic pegmatites in the Moldanubicum, Czech Republic: Primary vs. secondary compositional trends. Canadian Mineralogist, 36, 659–672.
——— (2001) Distinctive compositional trends in columbite-tantalite from two segments of the lepidolite pegmatite at Rožná, western Moravia, Czech Republic. Journal of the Czech Geological Society, 46, 1–8.
Novák, M., Černý, P., and Uher, P. (2003) Extreme variation and apparent reversal of Nb-Ta fractionation in columbite-group minerals from the Scheibengraben beryl-columbite pegmatite, Maršíkov, Czech Republic. European Journal of Mineralogy, 15, 565–574.
Novák, M., Černý, P., Cempírek, J., Šrein, V., and Filip, J. (2004) Ferrotapiolite as a pseudomorph of stibiotantalite from the Laštowičky lepidolite pegmatite, Czech Republic; an example of hydrothermal alteration at constant Ta/(Ta+Nb). Canadian Mineralogist, 42, 1117–1128.
Oliver, G.J.H., Corfu, F., and Krogh, T.E. (1993) U-Pb ages from SW Poland: Evidence for a Caledonian suture zone between Baltica and Gondwana. Journal of the Geological Society, 150, 355–369.
Pekov, I.V., Yakubovich, O.V., Shcherbachev, D.K., and Kononkova, N.N. (2003) The new columbite-tantalite group mineral from desilicated granite pegmatites of Lipovka (the Central Urals) and its genesis. Zapiski Vsesoyuznogo Mineralogicheskogo Obshchestva, 132(2), 49–59 (in Russian).
Pieczka, A. (2000) A rare mineral-bearing pegmatite from Szklary serpentinite massif, the Fore-Sudetic Block, SW Poland. Geologia Sudetica, 33, 23–31.
——— (2007a) Beusite and unusual Mn-rich apatite from the Szklary granitic pegmatite, Lower Silesia, Southwestern Poland. Canadian Mineralogist, 45, 901–914.
——— (2007b) Blue dravite from the Szklary pegmatite, Lower Silesia, Poland. Mineralogia Polonica, 32/8, 209–218.
Pieczka, A. and Gołębiowska, B. (2001) Altered pyrochlore from the Szklary rare-element pegmatite, Lower Silesia, Poland. In A. Piestrzyński et al., Eds, Mineral Deposits at the Beginning of the 21st Century. Proceedings of the Joint sixth Biennial SGA-SEG Meeting, 469–472, Kraków, Poland.
Pieczka, A. and Kraczka, J. (1996) X-ray and Mössbauer study of black tourmalines (schorls) from Szklary (Lower Silesia, Poland). Mineralogia Polonica, 27/2, 33–40.
Pieczka, A. and Marszałek, M. (1996) Holtite—the first occurrence in Poland. Mineralogia Polonica, 27/2, 3–8.
Pieczka, A., Marszałek, M., and Gołębiowska, B. (1997) Manganoniobite, stibioniobite and Hf-zircon from the Szklary pegmatite, Lower Silesia, (Poland). Mineralogia Polonica, 28/2, 89–100.
Pouchou, J.L. and Pichoir, F. (1985) "PAP" (phi-rho-z) procedure for improved quantitative microanalysis. In J.T. Armstrong, Ed., Microbeam Analysis, p. 104–106. San Francisco Press, California.
Pryce, M.W. (1971) Holtite: A new mineral allied to dumortierite. Mineralogical Magazine, 38, 21–25.
Shannon, R.D. (1976) Revised effective ionic radii and systematics studies of interatomic distances in halides and chalcogenides. Acta Crystallographica, A32, 751–767.
Timmermann, H., Parrish, R.R., Noble, S.R., and Kryza, R. (2000) New U-Pb monazite and zircon data from the Sudetes Mountains in SW Poland; evidence for a single-cycle Variscan Orogeny. Journal of the Geological Society, 157, 265–268.
Uher, P., Černý, P., Chapman, R., Határ, J., and Miko, O. (1998) Evolution of Nb,Ta-oxide minerals in the Prašivá granitic pegmatites, Slovakia. II. External hydrothermal Pb,Sb overprint. Canadian Mineralogist, 36, 535–545.
van Breemen, O., Bowes, D.R., Aftalion, M., and Żelaźniewicz, A. (1988) Devonian tectonothermal activity in the Sowie Góry gneissic block, Sudetes, southwestern Poland: evidence from Rb-Sr and U-Pb isotopic studies. Journal of the Polish Geological Society, 58, 3–10.
Voloshin, A.V. and Pakhomovskyi, Ya.A. (1988) Mineralogy of Tantalum and Niobium in rare-elements pegmatites. Nauka, Leningrad, Russia (in Russian).
Voloshin, A.V., Gordienko, V.V., Gel'man, Ye.M., Zorina, M.L., Yelina, N.A., Kul'chitskaya, K.A., Men'shikov, Yu.P., Polezhayeva, L.I., Ryzhova, P.I., Sokolov, P.B., and Utochkin, G.I. (1977) Holtite (first find in SSSR) and its relationship with other tantalum minerals in rare-metal pegmatites. Zapiski Vsesoyuznogo Mineralogicheskogo Obshchestva, 106(3), 337–347 (in Russian).
Voloshin, A.V., Pakhomovskiy, Ya.A., Puscharovskiy, D.Yu., Nadezhina, T.N., Bakhchisaraitsev, A.-Yu., and Kobyashev, Yu.S. (1989) Strontiopyrochlore: composition and structure. Trudy Mineralogicheskogo Muzeya AN SSSR, 36, 12–24 (in Russian).
Żelaźniewicz, A. (1990) Deformation and metamorphism in the Góry Sowie gneiss complex, Sudetes, SW Poland. Neues Jahrbuch für Geologie und Paläontologie, Abhandlungen, 179, 129–157.

Manuscript received June 17, 2009
Manuscript accepted May 1, 2010
Manuscript handled by Anton Chakhmouradian